NASA CONTRACTOR REPORT

NASA CR-1653

INVESTIGATION OF THE INFLUENCE OF DUCT-MOUNTED HELMHOLTZ RESONATORS ON THE SOUND FIELD OF A MODEL DUCTED PROPELLER

by David Brown

Prepared by
BELL AEROSPACE COMPANY
Buffalo, N.Y. 14240
for Langley Research Center

NATIONAL AERONAUTICS AND SPACE ADMINISTRATION • WASHINGTON, D. C. • SEPTEMBER 1970

1. Report No.	2. Government Accession No.	3. Re
NASA CR-1653		

4. Title and Subtitle	5. Report Date
INVESTIGATION OF THE INFLUENCE OF DUCT-MOUNTED HELMHOLTZ RESONATORS ON THE SOUND FIELD OF A MODEL DUCTED PROPELLER	September 1970
	6. Performing Organization Code
7. Author(s)	8. Performing Organization Report No.
David Brown	N/A
9. Performing Organization Name and Address	10. Work Unit No.
Bell Aerospace Company Buffalo, New York	11. Contract or Grant No. NAS1-8220
	13. Type of Report and Period Covered Contractor Report
12. Sponsoring Agency Name and Address National Aeronautics and Space Administration Washington, D.C. 20546	14. Sponsoring Agency Code

15. Supplementary Notes

16. Abstract

This study was basically an experimental investigation of the influence of wall-mounted Helmholtz resonators on the sound field of a ducted propeller, with an objective of determining the feasibility of far-field noise reduction. The investigation utilized two model propeller ducts, with an array of discrete resonator units installed at the wall surface.

Preliminary measurements, with the resonators tuned to the propeller harmonics, indicated a significant increase in the far field signature. An analytical model, illustrating the effect of wall impedance on dispersive acoustic modes, was then derived. This suggested a critical influence of the reactive impedance on the transmission loss (for a constant resistive impedance). Further experimental studies did not achieve the desired objective, but indicated the necessity for consideration of modal coupling, particularly to radial modes, if far field noise attenuation were to result.

17. Key Words (Suggested by Author(s))	18. Distribution Statement
Ducted propeller noise Helmholtz resonators Model propeller	Unclassified - Unlimited

19. Security Classif. (of this report)	20. Security Classif. (of this page)	21. No. of Pages	22. Price*
Unclassified	Unclassified	61	$3.00

*For sale by the Clearinghouse for Federal Scientific and Technical Information
Springfield, Virginia 22151

CONTENTS

TABLES

ILLUSTRATIONS

ILLUSTRATIONS (CONT.)

INVESTIGATION OF THE INFLUENCE OF DUCT-MOUNTED HELMHOLTZ RESONATORS ON THE SOUND FIELD OF A MODEL DUCTED PROPELLER

By David Brown
Bell Aerospace Company

SUMMARY

This study was basically an experimental investigation of the influence of wall-mounted Helmholtz resonators on the sound field of a ducted propeller, with an objective of determining the feasibility of far-field noise reduction. The investigation utilized two model propeller ducts, with an array of discrete resonator units installed at the wall surface.

Preliminary measurements, with the resonators tuned to the propeller harmonics, indicated a significant increase in the far field signature. An analytical model, illustrating the effect of wall impedance on dispersive acoustic modes, was then derived. This suggested a critical influence of the reactive impedance on the transmission loss (for a constant resistive impedance). Further experimental studies did not achieve the desired objective, but indicated the necessity for consideration of modal coupling, particularly to radial modes, if far field noise attentuation were to result.

INTRODUCTION

The ducted propeller system, as utilized on V/STOL vehicles and ground-effect machines, comprises a single rotor, of low blade number, contained within a cylindrical airfoil duct with well separated stators and no inlet guide vanes. For a specific required thrust, a system design can be optimized to achieve relative sound reduction by minimizing the propeller rotational tip-speed, particularly to the low subsonic range ($M < 0.6$). In this range, the discrete-frequency sound generated by the propeller is

transmitted to the duct inlet and efflux cross sections by dispersive acoustic modes. The far-field sound pressures radiated from the duct extremities depend not only on the sound power at these sections, but also on the spatial distribution of the appropriate mode particle velocity and phase (Refs. 1, 2, and 3).

This study resulted from a series of experiments, to determine methods of achieving noise reduction in ducted-propeller systems. As the predominant sound field is of a discrete-frequency nature, the application of a tuned resonator array appeared to be most applicable. Subsequent experiments in a model duct with a loudspeaker excitation at representative frequencies, indicated that a substantial attenuation could be achieved. The present study is an extension of that work, with the excitation provided by a three-blade propeller located at approximately the 40% chord point of the duct.

While the principles of transmission loss by sidebranch resonators have been studied for some time (e.g., Ref. 4), the recent works of Ingard, Ising, Blackman, Phillips, Garrison and Marino et al (Refs. 5 through 10) have provided an insight to the nonlinear effects at high incident sound pressures, allowing application to turbofan and similar systems. The influence of cross-flow velocity on the resonator performance has also been studied in some detail in Refs. 8 and 11.

Among the applications to the high-order modes of ducts is that by Copeland (Ref. 12) who achieved a reduction of 10 dB at the fundamental blade passage frequency of a compressor stage. More recent studies are summarized in Ref. 13, and a work of some considerable interest to the present study is Ref. 14.

The work reported herein comprises a study of a matrix of resonator designs, suitable for installation on 1/6 scale ducted-propeller units, and the acoustic characteristics of these units relative to the generated sound field, the boundary conditions of the duct wall, and the far-field radiated sound pressure spectra. The experimental arrangement is described, and an analytical model of the system is derived, with comparison of theoretical and measured results.

SYMBOLS

a	outer-duct radius
A	cross-sectional area
b	inner-duct radius (hub)
B	number of propeller blades
c	sonic velocity
d	orifice diameter
f	frequency
J_{MB}	Bessel function of first kind, of order (M x B)
K	wave number
L	duct length
m,n	harmonic numbers in circumferential and radial modes, respectively
N	rpm of propeller
p	sound pressure
r, θ, x	cylindrical coordinates of duct
R	specific acoustic resistance
S	surface area of duct wall
SPL	sound pressure level, dB re 2×10^{-4} microbar
t	orifice thickness
u	particle velocity
U	duct flow velocity
V	resonator cavity volume
X	specific acoustic reactance
Z	specific acoustic impedance ($= R + i X$)
α	absorption coefficient
γ	ω/ω_o
η	angle of boom-microphone orientation
ζ	normalized specific acoustic impedance ($= \theta + i \chi$)
λ	wavelength

μ coefficient of viscosity

ρ density of air

σ , τ axial transmission exponents

ϕ azimuth angle from thrust vector, external to duct

ω radian frequency

θ normalized specific acoustic resistance

χ normalized specific acoustic reactance

Subscripts

o orifice

e effective

res resonance

w wall

EXPERIMENTAL ARRANGEMENT

Propeller Ducts and Test Facilities

Design and fabrication of ducts. - Two pairs of model propeller ducts were manufactured, each pair having a different chord length. The internal diameter of the ducts was 16 in. Each duct could be mounted to a variable-speed (electric motor) power unit with a flexible-coupled drive to the propeller. The ducts are solid wall, of casting resin molded to a 1/8-in. aluminum liner. One of each pair was employed as a reference duct to provide basic sound field definitions, the other two ducts being modified to incorporate resonator units. The basic duct geometries are as shown in Figure 1, and the modified resonator ducts are shown in Figure 2. Details of the duct modification and the resonator designs are shown in exploded view in Figure 3. The total number of resonators in the duct wall was mainly determined by the resonator cavity diameter and the separation required by the method of mounting. The cavity diameter was fixed as that which would allow adequate volume tuning range for the propeller harmonic frequencies without inducing standing waves over the cavity depth. Taking

account also of the requirement for maximum open area ratio on the duct wall surface, a staggered resonator array was derived, with 18 resonators per circumferential row. This allows a maximum of 90 and 126 units to be mounted on the short and long duct, respectively.

Instrumentation and analysis facilities. - The arrangement of the ducted propeller test stand within the anechoic facility is illustrated in Figure 4. Three high-intensity pressure transducers were used to measure the sound pressures at the duct wall and in the resonator cavities. Spatial, in-duct distribution of the sound field was measured by a 1/4-in. diameter condenser probe microphone with windshield. The external sound field measurements were obtained by two screened, 1/2-in diameter condenser microphones, mounted on a remote-controlled rotary boom, at radii of 5 ft and 10 ft from the propeller disc center. Two tripod-mounted microphones were also available for "far-field" measurements outside the boom radius. Analysis of the sound fields was carried out by on-line frequency analyzers with constant percentage bandwidth capability from 6% to octave. A multichannel tape recorder was available for permanent-record acquisition of sound pressure histories. The instrumentation package is further defined schematically in Figure 5.

Anechoic facility. - Referring again to Figure 4, the facility used as a measurement chamber was of dimensions 40 ft by 30 ft, by 15 ft high. The walls and ceiling were covered by a 5-in. acoustical blanket and the floor covered by a 3-in. blanket of similar material.

Resonator Design Study Facilities

Impedance tube. - The evaluation of nonlinear characteristics due to high sound pressure levels was conducted by the impedance-tube method, as defined in Ref. 15, in a facility fabricated for rocket engine stabilizing studies. The tube is of circular cross section having a 4-in. diameter, and is approximately 3 ft long, containing a 30° elbow bend at the sound-source end. Sound power is supplied by a 100-W electromagnetic transducer, with discrete frequency control by a beat-frequency oscillator. In each

test, the termination sample consisted of a rigid end plate with single orifice and attached resonator cylinder. The travelling microphone is a 1/2-in. diameter condenser type and is connected to a narrow-band frequency analyzer and power supply.

Traveling-wave tube. - In order to assess the influence of cross-flow velocity on the resonator performance, a simple travelling-wave tube was manufactured which would allow air flow velocities of up to 100 fps, and sound pressure levels of 150 dB (discrete frequency). The tube is 4.625 in. square, 8 ft in length and terminated by a flat, exponential horn and anechoic duct section. At the source end, an electromagnetic or electropneumatic sound source can be installed at one end of a Y-branch connector, while air flow is introduced at the other branch. Resonators and/or microphones can be installed at equidistant locations along the duct length. Air flow measurements can be obtained over the duct cross section by a traversing pitot-static tube arrangement.

RESONATOR DESIGN STUDIES

General

The basic objective of this study requires the design of a lattice array of resonator units, mounted at the propeller duct wall, tuned to the rotational sound harmonic frequencies, and optimized in terms of the effective absorption coefficient and sound attenuation. The method of installation shown in Figure 3 imposes certain restrictions on the resonator geometries, and the following design studies are based on practical orifice sizes which allow a range of resistive impedances and tuned frequencies to be examined. As the expected sound pressure levels and air flow velocities in the model ducts are in the range 100-140 dB and 100 fps, respectively, a study of nonlinear effects on the resonator impedance is essential.

Resonator Theory

The impedance terminology used here is that employed by Ingard (Ref. 5). That is, the specific acoustic impedance is given by

$$\left.\begin{aligned} Z &= R + iX = \rho c\,(\theta + i\chi) \\ R &= 4\,R_S\,(1 + t/d + \Delta_{NL}/d) \\ X &= (\rho\omega\ell_e - \rho c^2 A_o/\omega V) \end{aligned}\right\} \qquad (1)$$

where

- d, t are the orifice diameter and orifice thickness, respectively
- ℓ_e is the effective orifice thickness
- $A_o = \pi d^2/4$
- V is the resonator cavity volume
- $R_S = 1/2\,(2\mu\rho\omega)^{1/2}$ is the surface resistance of the orifice (due to viscosity)
- Δ_{NL}/d is an empirically derived term which acts as a "nonlinear correction" on the resistive impedance
- ω is the excitation radian frequency

From the reactive impedance, the resonant frequency is derived as

$$\omega_o = c\left[A_o/V\ell_e\right]^{1/2} \qquad (2)$$

and the normalized specific reactance can be rewritten as

$$\chi = k_o\,\ell_e\,(\gamma - 1/\gamma) \qquad (3)$$

where $\gamma = \omega/\omega_o$, $k_o = \omega_o/c$

For a lattice area of resonators in a wall, excited by a plane wave normal to the wall, the effective wall impedance is expressed (approximately) by Ingard and Ising (Ref. 6) as

$$\theta_w + i\chi_w = \theta/\sigma_1 - i\chi/\sigma \qquad (4)$$

where $\sigma_1 = \sigma/(1-\sigma^2)$

σ = open area ratio at wall surface,

and the normal incidence absorption coefficient is

$$\alpha_w = 4\theta_w \Big/ \left\{ \left[\theta_w + 1 \right]^2 + \chi_w^2 \right\} \tag{5}$$

As little is known about the interference effects of the resonators in an array, the above absorption coefficient can only be considered as the maximum attainable, provided the lattice spacing is much less than the half wavelength of the incident wave.

In the above expressions, the design variables are obviously d, t, V and σ. The parameters, ℓ_e and Δ_{NL}/d, require definition. The effective orifice thickness is defined by (Ref. 5)

$$\ell_e = t + 0.85\, d\, (1 - 0.625\, d/d_c) \tag{6}$$

where d_c = cylinder diameter

The nonlinear resistance correction term, Δ_{NL}/d, has received considerable experimental study (for rocket combustion-chamber liner application) at high sound pressure levels, but with large discrepancies in the comparative definitions, as summarized in Ref. 8. Consequently, for the present study this term is experimentally evaluated for resonator designs applicable to the model duct.

One other expression employed in subsequent analysis is that which relates the measured sound pressure gain, between the wall surface and the resonator cavity, and the resonator resistive impedance:

$$G = \text{Gain (dB)} = 20 \log_{10} \left| p_c/p_i \right|$$

where

p_c is the cavity sound pressure

p_i is the incident field sound pressure

Now $p_c/u_o = \rho c^2 A_o/i\omega V$

and $p_i/u_o = \rho c (\theta + i\chi)$

where u_o is the particle velocity close to the orifice

Therefore,

$$G = 20 \log_{10} \left[A_o/K V (\theta^2 + \chi^2)^{1/2} \right] \text{dB} \tag{7}$$

At resonance,

$$G = 20 \log_{10} \left[A_o / K V \theta \right] \text{ dB} \qquad (8)$$

The above relationships are used in three phases of the present study. Initially, they allow a definition to be obtained for the effective length of the orifice, and the nonlinear resistance in terms of resonator geometry, frequency and incident field characteristics. This forms a basis for the resonator designs utilized in the model-duct program. In subsequent application studies, the resonator orifice and cavity depth settings are varied to allow an impedance effect study, and the theoretical relationships are necessary to define the operating characteristics of the resonators.

Experimental Studies

Impedance-tube tests. - A set of prototype resonators, of cylindrical geometry as shown in Figure 3, were manufactured for study in the impedance tube. Various orifice discs, with aperture dimensions listed below, were employed in this study.

Orifice diameter (in.)	0.187	0.250	0.312	0.375	0.375	0.516	0.625
Orifice depth (in.)	0.250	0.250	0.250	0.187	0.250	0.187	0.125

The resonator cavity depth could be varied to allow tuned frequencies in the range 350-1200 Hz to be attained, with the restriction that the depth would not exceed one-sixth of a wavelength. Due to the size of the impedance tube (4-in. diameter), resonator units were installed individually at the termination section, and the impedance was evaluated by the procedures defined in Ref. 15. Discrete-frequency excitation levels of 90, 110, and 130 dB sound pressure level (SPL) were induced at the resonator orifice plane, at frequency increments of 10 Hz through resonance.

From the impedance data obtained in each resonator test, the nonlinear resistance correction term (Δ_{NL}/d) and the orifice effective length (ℓ_e) were evaluated by substitution in the theoretical equations for the normalized specific resistance and the resonant frequency.

The dependence of Δ_{NL}/d on the sound pressure level is shown in Figure 6 for each of the resonators. As these data points were obtained for resonators of different aperture dimensions and different tuned frequency, a linear relationship between Δ_{NL}/d and the sound pressure can be assumed to give a sufficient definition of the resistive impedance for the present application. This is derived from the data as

$$\log_{10} (\Delta_{NL}/d) = 0.0322 \text{ SPL} - 3.09 \quad (9)$$

and is compared in Figure 6 with similar relationships derived in other literature (Refs. 5, 7, and 8).

The resonant frequency was found to be estimated within 4% accuracy by the effective length definition of equation (6), except for the two largest-diameter orifices (0.516-in. and 0.625-in. diameter) where the error was in the order of 10%. A brief analysis of these errors indicated that the effective length is better defined by

$$\ell_e = t + 0.85\, d \quad (10)$$

for the larger apertures, the resonant frequencies being within 2% of the modified estimates.

The above studies of the resonator impedance characteristics allowed an estimation to be made of comparative absorption coefficients in a propeller duct application. At this phase of the program, the fabrication of the ducts was not completed, and assumptions were therefore made for the expected sound field frequencies and harmonic levels. Employing equations (1), (4), (5) and the empirical relationship (9), the resonance absorption coefficients of arrays of tuned resonators with fixed spacing (as defined in Figure 3) but different orifice dimensions were calculated for a propeller rotational speed of 8000 rpm (giving harmonic frequencies of 400, 800, and 1200 Hz). The resultant estimates are presented in Table I for each of these harmonics, assuming 130 and 140 dB SPL, respectively, for the fundamental, and a spectral decay of 10 dB per harmonic. These results indicated that a single orifice design would not provide optimum absorption at all resonance frequencies. It was therefore decided to manufacture, in quantity for duct application, sets of orifice discs with 0.375-in. aperture

diameter, and 0.25- and 0.187-in. thickness. The 0.625-in. diameter, 0.125-in. thick apertures were incorporated in the duct aluminum liner.

Travelling-wave tests with air flow. - As a further guide to the response of resnators in the propeller-duct environment, a simple travelling-wave tube was manufactured, in which air flow velocities of up to 100 fps could be induced. Preliminary reference measurements in this facility indicated the presence of axial standing waves, which were minimized by modification of the termination horn and absorptive duct. However, it was apparent that these standing wave effects precluded a useful evaluation of the resonator effective impedance over the frequency range of interest. The results of these tests were therefore regarded as only indicative of the influence of air flow velocity, and are summarized in Figure 7.

In each test, with and without air flow, two resonators were installed in the wall with 2-in. axial separation. Microphones were flush-mounted at three locations downstream and two locations upstream of the resonators. A discrete-frequency signal was superimposed on the random noise field to give 130 dB SPL at an upstream microphone location, and all other measurements were taken relative to this level. The axial distribution of sound pressure level was measured first with the resonant orifices blocked, and then with the resonators active. The signal frequency was changed by 10-Hz increments through resonator resonance. The downstream insertion loss is considered as the measured difference in sound pressure level at the downstream microphones due to the resonators' influence. The data presented in Figure 7 are the maxima over each frequency scan. The transmission loss data of Figure 7 are the corresponding differences between upstream and downstream microphone levels.

These experiments indicate that at zero flow velocity the greatest attenuation is provided by the larger-diameter orifices. However, as the air flow velocity is increased, the degradation of attenuation is more prominent as the orifice diameter is increased. This effect has been investigated in Ref. 11 and may be attributed to an induced turbulence at the orifice with consequent modification of the orifice resistance and effective mass. It was concluded from these tests that at flow velocities and sound pressure

levels representative of that expected in the propeller duct the orifice diameter may be increased to about 0.375 in., with resultant increase in resonator effectiveness.

An observation made during the above studies, which is of some importance in the propeller duct tests, is that an increase of the downstream sound level was not experienced during the frequency scans over the air flow velocity range.

DUCTED-PROPELLER TEST PROGRAM

Reference-Duct Sound Surveys

Each of the reference propeller ducts described in Figure 1 was installed in the test facility, and preliminary sound-field surveys were made at various operating conditions of propeller rotational speed and blade angle. The objectives of these tests were: (a) to obtain operating conditions at which the rotational harmonic sound levels would be well defined, relative to the broadband level and auxiliary-system level, at the boom microphones, and (b) to obtain a spatial definition of the harmonic levels, in the duct and at the boom microphone radii, to be employed as reference data in the resonator application program. The facility arrangement for these tests is illustrated in Figure 4. The locations and nomenclature of the microphones installed within the ducts and on the rotary boom are defined in Figure 8.

The range of operation of the model system was basically defined by the theoretical performance data of Figure 9 and by the practical limitations of the system. With the short-chord duct (duct No. 1) installed, preliminary sound surveys were carried out at the 10-ft radius boom microphone for propeller operating conditions of 4000, 6000, and 8000 rpm, with blade-angle settings of 15, 20, and 25 degrees. These surveys indicated a requirement for the highest blade-angle setting, and propeller speeds greater than 4000 rpm, to achieve an adequate definition of the rotational sound harmonic levels at the boom microphones. A comparison of the measured spectra for the three rotational speeds (at the 25° blade-angle setting) is shown in Figure 10.

The above procedure was repeated with the longer-chord duct (duct No. 2) installed. In this case it was found necessary to operate at 8000 rpm, with the 25° blade-angle setting.

Reference sound spectra were then obtained at 6000 and 8000 rpm for duct No. 1, and at 8000 rpm for duct No. 2. These spectra comprise 6% bandwidth analyses of sound pressure histories at the following locations:

(a) Duct-wall transducer positions (K).

(b) Boom microphones, B2 and B3 (at 10-ft and 5-ft radii, respectively) at 30° increments in the horizontal plane through the propeller axis.

(c) Probe-microphone locations (B1) in the duct upstream of the propeller, at specified cylinder coordinates relative to the propeller disc.

The data of Table II are compiled from the spectra measured at the duct wall and at the boom locations. This tabulation shows the harmonic levels at the propeller rotational frequencies. Corresponding data, measured at probe microphone locations within the duct, are plotted relative to location in Figures 11, 12, and 13. (The limitation of data in duct No. 1 was due to the arrangement of the drive shaft upstream of the propeller in the original propulsion test stand. This was later modified to accommodate long duct No. 2 in a reversed position.)

As the measured axial decay rates are shown in Figures 11 and 12 to change at some distance from the propeller plane, the theoretical slopes for the m^{th} tangential, n^{th} radial acoustic modes are superimposed on these figures for comparison. For each harmonic, the three most significant modes are considered. The estimation procedure is defined in Appendix A.

A comparison of the theoretical and measured characteristics of the reference-duct data and reference to the radial distributions of Figure 13, offer the following conclusions regarding the reference-duct sound field:

(a) The rotational sound field generated by the propeller is transmitted along the duct by dispersive acoustic modes.

(b) Both tangential and radial modes are significant at sections close to the propeller. At the duct leading-edge section, radial modes may be predominate due to their lower decay rate.

(c) The second and third propeller harmonics are radiated to the far field with a higher radiative efficiency than the fundamental component. This may be attributed to the modal content at the duct leading-edge section.

Resonator Impedance Studies

The reference ducts described in the preceding section were replaced by modified ducts, of identical geometry, with an array of 0.625-in. diameter apertures distributed over the wall surface backed by threaded cylindrical cavities for resonator installation. Details of the modifications are shown in Figure 3.

To obtain a more appropriate definition of the resonator response characteristics than that estimated in impedance-tube tests, a series of impedance studies were conducted with the resonators installed in the modified ducts and subjected to the actual operating environment of the propeller-duct system.

These studies were implemented by measuring the sound pressure gain (dB) between a transducer mounted at the duct wall and a transducer mounted in the resonator cavity wall. With an array of identically tuned resonators installed in the duct wall, the propeller rotational speed was increased by small increments through a specified range, such that the resonators would be excited through resonance by the propeller harmonics. For example, with the resonator units tuned to 600 Hz the following propeller speeds were employed:

Propeller rpm	Harmonic Number	Harmonic Frequency (Hz)
5500-6500	2	550-650
3600-4400	3	540-660
2800-3300	4	560-660

Each speed range provided resonator-gain measurements for different incident sound levels and air flow velocities. This procedure was repeated for two sets of orifice discs,

with resonator frequencies in the order of 600 and 900 Hz. Typical results of these tests are presented in Figure 14.

For simplicity, the maximum measured gain was assumed to occur at resonance, and this gain was converted to a resistive impedance value for each resonator by substitution in equation (8) of the resonator-design theory. The nonlinear resistance correction term (Δ_{NL}/d) was then evaluated for each test and related to the incident sound pressure level as shown in Figure 15. A comparison of this data with that obtained from the impedance-tube tests, also shown in Figure 15, indicates that equation (9) overestimates the nonlinear correction term by about 40%. At high sound pressure levels (where ($\Delta_{NL}/d) >> (1 + t/d)$), this error would be reflected in the estimated impedance. The influence on the absorption coefficient must be calculated for each orifice. Consequently, equation (8) is replaced by

$$\log_{10} (\Delta_{NL}/d) = 0.0289 \text{ SPL} - 2.79$$

which is derived from Figure 15, for estimation of the resonator impedance in later test phases.

An accurate assessment of the resonance frequency of the resonator unit was attempted by phase measurement between the transducer signals. As a phase difference was expected in the circumferential direction at the duct wall, an attempt was made to obtain a correction term, allowing for the transducer displacement from the orifice. This correction term could not be determined with sufficient accuracy because of significant oscillatory changes in the phase relationship between two wall-mounted transducers at the test conditions.

The resonance frequency was therefore assumed to correspond to that at the maximum sound pressure gain measured over the resonator. The air flow velocity at a radial distance of 1 in. from the resonator orifice was measured in each test by a pitot-static tube arrangement. A comparison of the estimated and measured resonance frequencies is shown in Table III together with the measured incident sound pressure levels and air flow velocity. From this comparison it was concluded that the effective orifice length is best defined by $\ell_e = t + 0.85\ d$ for each of the aperture sizes considered.

Resonator Application Studies

General. - This section reports the results obtained in sound surveys of the modified propeller-duct system, with resonator arrays applied to the duct wall. The application program was conducted in three phases:

(a) All resonator units in the array were identically tuned, to a frequency corresponding to one of the propeller sound harmonics. This was repeated for different harmonics.

(b) Resonators tuned to different harmonic frequencies were arranged in a staggered distribution over the array.

(c) With all resonators identically tuned, the resonance frequency was incrementally changed through a range encompassing the harmonic frequencies.

In each test the sound pressure spectra, at the wall-mounted transducers and at specific azimuth locations of the boom microphones, were evaluated and compared with the corresponding reference-duct data. A spatial survey of the harmonic levels inside the duct was conducted for a representative test case.

The transducer locations and nomenclature are as defined for the reference tests. The superscript (r) is employed to denote measurement of the sound pressure in the resonator cavity.

Uniform arrays - tuned to propeller harmonics. - These tests were carried out at propeller speeds of 6000 rpm and 8000 rpm, at which the rotational sound frequencies were 300, 600, 900. . . . . .Hz, and 400, 800, 1200. . . . . .Hz, respectively. Spectral measurements of the sound field at various transducer locations were taken for different resonator settings and compared with the reference-duct data. The change in the harmonic levels due to resonator installation is presented in Table IV for each of the test cases.

The significant increase in sound pressure level at the boom microphones was contrary to the expected influence of the resonators. A survey of the sound levels along the duct-wall outer surface was carried out after the initial tests, to ensure that the resonators did not radiate a significant level through the cavity walls. These levels

were found to be of the same order of magnitude as the boom measurements, thereby eliminating wall radiation as a major source.

From the tabulated increments in harmonic levels it is apparent that the 800-Hz and 900-Hz components, at 8000 rpm and 6000 rpm, respectively, are influenced to the greatest extent by the resonators. As these frequencies are in the region of the radial-mode frequency (1020 Hz), it was concluded that this mode is amplified by the wall resonators. The higher harmonics, above the cut-off frequency, will also propagate in this mode, as indicated by Tyler and Sofrin (Ref. 1). For one test case, a radial scan of the first three harmonic components was obtained at a section near the duct leading edge using the probe microphone. The results are shown in Figure 16. This scan was taken in a plane through a resonator row. Comparison with results obtained in the reference duct shows a 12 dB increase in the tuned frequency component close to the resonator orifice. This difference diminishes to 4 dB at 2.5 in. from the wall orifice and increases again to 15 dB as the duct center line is approached. This suggests that the driven resonators radiate energy, which is concentrated towards the duct center in a radial mode pressure distribution.

The premise upon which this study was originally based, that the resonator influence would be of a dissipative nature, can apparently be discarded in favor of a dispersive field analysis. That is, the boundary conditions at the duct wall, as defined by the resonator array, are modified in such a manner that the transmission of each mode is modified. As these modes are dispersive in the propeller duct, the influence of boundary conditions on the axial decay rates requires some resolution. A theoretical study of these effects was initiated at this phase of the program, and is presented in Appendix A. Further reference to this is made in a later section.

Staggered resonator arrays. - The array of resonators in duct No. 1 was arranged such that no adjacent units were tuned to the same frequency, and a test case was evaluated at 8000 rpm. The resonator tuning frequencies were 400 Hz, 800 Hz, and 1040 Hz.

Further tests were conducted with the resonators arranged in three sets around the duct circumference, each set having a different tuned frequency. This test was repeated with an absorptive material (fiberglass) in the resonator cavities.

These tests were conducted to investigate the possibility that interaction between adjacent resonators contributed to the gain in the sound field, and to determine whether an assymmetric resonator arrangement would influence the suspected radial-mode contribution.

As is shown in Table V, the harmonic levels measured at the boom locations were above the reference data, particularly in the second and higher harmonic components.

The addition of fiberglass to the resonator cavities resulted in a further increase in the third and higher harmonics. An explanation of these results has not yet been resolved.

Uniform arrays - scanned tuning. - At this stage of the program, the theoretical work of Appendix A was completed and a series of tests was carried out to evaluate the implications of the theory. Basically, the analysis assumes a complex wall impedance which is spatially continuous and locally reactive. The influence of this wall impedance on the cut-off wave number of each acoustic mode is evaluated numerically, and the resultant change in the axial-transmission factor is calculated.

For the present program, the primary result of the above study is the apparent variation of the axial decay factor about the rigid-duct value. At some small positive-reactive wall impedance, the analysis suggests that the decay exponent will be equal to the rigid-duct value. Lower, or negative, reactance will induce a high decay, while an increased positive reactance will cause the decay exponent to diminish to some minimum value and then to increase asymptotically to the rigid-wall value.

In the actual duct, the resonators were tuned in previous tests to the propeller harmonics. This means that the reactance at each orifice is zero. However, as the incident wave is not a plane wave, and a phase difference is known to occur in the circumferential direction, the effective wall impedance of the array cannot be simply

regarded as being zero-reactive at resonator resonances. If this effective reactance is positive, the experimental results of the earlier tests might be attributed to the boundary condition effects shown in Appendix A.

A test series was consequently carried out to determine whether a wall-impedance condition could be achieved which would provide an increased transmission loss within the duct for the rotational sound harmonics. In these tests the propeller speed was fixed at 8000 rpm, and the resonator cavity depth was incremented through the available range. At each setting, a measurement of each sound harmonic level at the duct wall and boom-microphone locations was recorded. This procedure was conducted for two orifice sizes.

The experimental results of this series are shown in Table VI and Figure 17.

It is apparent that the experimental results do not conform to the relationships derived in the theoretical model. The coupling between the radial and circumferential modes of the duct, ignored in the theory, is apparently strengthened by the resonators, with a resultant change in the radial distribution of sound pressure at the duct leading-edge section.

Summary. - A test program has been carried out to evaluate the influence of various resonator arrays on the sound field of a model propeller-duct system. The results of this program show the far-field sound levels to be higher than corresponding measurements of a rigid-wall reference-duct system. The reference far-field spectra show the second and higher harmonics to be of greater amplitude than the fundamental, and these higher harmonics are shown to be influenced to the greater extent by the resonator arrays.

A survey of the in-duct sound field, with varied resonator tuning, indicates that the radial pressure distribution of these higher harmonics is significantly changed by the resonators, with increased levels occurring predominantly at the duct center and duct wall. This is interpreted as due to a radial-tangential mode coupling at the wall boundary, with the radial-mode frequencies being modified towards a coincidence with the excitation (propeller-harmonic) frequencies.

A further diagnostic analysis of these results was not anticipated at the study commencement, and is therefore outside the scope of this report.

CONCLUSIONS

1. The installation of Helmholtz resonators on the wall of a model propeller duct has been noted to modify the harmonic content of the sound field within the duct, such that a significant increase in the far-field harmonic levels results.

2. The interaction between the resonator arrays and the propeller-duct sound field is of a more complex nature than was originally anticipated. Inter-mode and resonator-acoustic mode coupling have a critical influence on the radiated sound field.

3. Surveys of the spatial distribution of sound pressure within the ducts suggest that for propeller harmonics which are in the frequency vicinity of radial acoustic modes the resonators couple these radial modes to the excitation harmonics. The radial modes have a greater radiation efficiency at the duct extremity.

4. An analytical study of the influence of a complex wall impedance on uncoupled, dispersive, acoustic modes of a duct suggests that the axial-decay exponent of the mode can be decreased (relative to the rigid-duct exponent) by a range of positive acoustic reactance values.

5. The initial assumption of a predominantly dissipative influence of resonator arrays on the duct sound field was not confirmed during this study.

6. The present study has indicated a requirement for a more detailed investigation of boundary conditions induced by resonator arrays in a cylindrical duct, and the influence of these conditions on the modal distribution of sound energy.

7. Within the scope of this study, it may be concluded that resonator arrays should not be applied, for noise reduction purposes, to axial fan systems with radial mode frequencies in the fan excitation frequency range. As the model ducted-propeller

system could not be operated outside the range of radial mode influence, a conclusion as to the influence on full-scale systems could not be made.

APPENDIX A

Ducted-Propeller Sound Transmission Theory

A simplified approach to the evaluation of wall-impedance effects on the sound transmission properties of a propeller duct is presented. The predominant acoustic transmission modes in the duct are studied individually, thereby neglecting coupling, and are assumed to be of tangential order (m) corresponding to blade number harmonics ($m = jB$, $j = 1, 2 \ldots\ldots$) and low radial order ($n = 0, 1$).

The cylindrical form of the modal solutions to the linear wave equation, with zero flow velocity, is assumed to be adequately expressed by

$$p_{mn}(r, \theta, x, t) = A_{mn} \cos(m\theta + \phi_{mn}) J_m(K_{mn}^{(r)} r) \cdot \exp\left[i(K_{mn}^{(x)} x - \omega_m t) \right] \tag{A1}$$

where

$$\omega_m = 2\pi f_m = 2\pi m N_p/60$$

$$K_m = \omega_m/c = \left[(K_{mn}^{(r)})^2 + (K_{mn}^{(x)})^2 \right]^{1/2}$$

As the cut-off wave number ($K_{mn}^{(r)}$) is known to be greater than K_m for a propeller with subsonic tip speed (Ref. 1), the exponent in the above expression may be rewritten as

$$i(K_{mn}^{(x)} - \omega t) = -i\omega_m t - \left[(K_{mn}^{(r)})^2 - (K_m)^2 \right]^{1/2} \cdot x$$

$$= -i\omega_m t - (\sigma_x + i\tau_x) \cdot x$$

The axial transmission loss is, therefore, TL = 8.68 σ_x dB per unit length.

The effect of wall impedance on this transmission loss is derived through the boundary condition imposed on equation (A1) at r = a.

That is, for a wall-surface specific acoustic impedance

$$Z_w = \rho c (\theta_w + i \psi_w) = \left[\frac{p_{mn}(r)}{u_{mn}(r)} \right]_{r=a} \tag{A2}$$

the particle velocity normal to the wall is

$$\left[u_{mn}(r) \right]_{r=a} = \frac{1}{i \rho c K_m} \left[\frac{\partial p_{mn}}{\partial r} \right]_{r=a} \tag{A3}$$

Substitution of (A1) and (A2) into (A3) gives the characteristic equation for $K_{mn}^{(r)}$:

Letting $\bar{\alpha}_{mn} = K_{mn}^{(r)} a$,

$$\frac{\partial}{\partial (\bar{\alpha}_{mn})} \left[J_m (\bar{\alpha}_{mn}) \right] - \frac{i K_m a}{\theta_w + i \psi_w} \cdot \frac{J_m (\bar{\alpha}_{mn})}{\bar{\alpha}_{mn}} = 0$$

This is solved numerically to give $\bar{\alpha}_{mn}$ for a given wall-surface specific acoustic impedance, and subsequently σ_x and the transmission loss are evaluated.

This procedure was translated to computer-program form, and the following input parameters were inserted:

For model propeller ducts,

Duct radius	a = 0.667 ft
Blade number	B = 3
Propeller rpm	N_p = 8000
Mode order	m = 3, 6, 9 (= jB)
	n = 0, 1

Normalized specific wall resistance range

$0.1 < \theta_w < 2.0$ (and ∞ for a rigid wall)

Normalized specific wall reactance range

$-1.0 \leq \psi_w \leq 1.0$ (and ∞ for a rigid wall)

Transmission loss for a rigid-wall duct was first estimated, and the difference due to finite wall impedance was obtained by comparison. The results of this analysis are presented in Figures 18, 19, and 20.

REFERENCES

1. Tyler,J.M. and Sofrin, T.G.: Axial Flow Compressor Noise Studies, S.A.E. Meeting Preprint 345 D, 1961.
2. Morfey, C.L.: Rotating Pressure Patterns in Ducts, J. Sound Vib. 1, 1964, pp. 60-87.
3. Fricke, W. and Bissel, J.R.: Analytical and Experimental Studies of the Sound Field in a Propeller Duct, J. Acoust. Soc. Am., Vol. 44, No. 5, 1968, pp. 1184-1188.
4. Steward, G.W.: Acoustic Transmission with a Helmholtz Resonator or an Orifice as a Branch Line, Phys. Rev., Vol. 27, 1926, pp. 487-493.
5. Ingard, Uno: On the Theory and Design of Acoustic Resonators, J. Acoust. Soc. Am., Vol. 25, No. 6, 1953, pp. 1037-1061.
6. Ingard, Uno and Ising, Hartmut: Acoustic Nonlinearity of an Orifice, J. Acoust. Soc. Am., Vol. 42, No. 1, 1967, pp. 6-17.
7. Blackman, A.W.: Effect of Nonlinear Losses on the Design of Absorbers for Combustion Instabilities. ARS J., Vol. 30, 1960, pp. 1022-1027.
8. Phillips, B.: Effects of High Wave Amplitude and Mean Flow on a Helmholtz Resonator, NASA-TM-X-1582, 1968.
9. Garrison, G.D.: A study of the Suppression of Combustion Oscillations with Mechanical Damping Devices, Pratt and Whitney Aircraft, PWA FR-2596, 1967.
10. Marino, P.A., Jr., Bohn, N. and Garrison, G.D.: Measurement of Acoustic Resistance at Sound Pressure Levels to 171 dB, J. Acoust. Soc. Am., Vol. 41, No. 5, 1967, pp. 1325-1327.
11. Mechel, F. and Schilz, W.: Research on Sound Propagation in Sound-Absorbent Ducts with Superimposed Air Streams. AMRL-TDR-62-140, Vols. I-IV, 1962.
12. Copeland, W. Latham: Inlet Noise Studies for an Axial Flow Single-Stage Compressor, NASA TN D-2615, 1965.
13. Conference: Progress of NASA Research Relating to Noise Alleviation of Large Subsonic Jet Aircraft, NASA SP-189, 1968.

14. Rice, Edward J.: Attenuation of Sound in Soft-Walled Circular Ducts. NASA paper, presented at Symposium on Aerodynamic Noise (Toronto, Canada), May 20-21, 1968.

15. Anon.: Standard Method of Test for Impedance and Absorption of Acoustical Materials by the Tube Method, ASTM C: 384-58, 1958.

TABLE I

ESTIMATED ABSORPTION COEFFICIENTS FOR PROPELLER DUCT WITH RESONATORS

Resonance Frequency (Hz)		400	800	1200	400	800	1200
Incident SPL (dB)		140	130	120	130	120	110
d (in.)	t (in.)	α_w			α_w		
0.250	0.250	0.51	0.62	0.78	0.76	0.85	0.93
0.375	0.250	0.81	0.92	0.99	0.98	0.99	0.97
0.375	0.187	0.82	0.92	0.99	0.99	0.97	0.96
0.516	0.187	0.98	0.99	0.94	0.96	0.88	0.76
0.625	0.125	0.99	0.95	0.82	0.85	0.74	0.60

α_w = wall absorption coefficient at resonance

d = orifice diameter (in.)

t = orifice thickness (in.)

SPL = sound pressure level at wall (dB re 2×10^{-4} μ bar)

NOTE: These estimates are for assumed sound pressure levels at the propeller-frequency harmonics.

TABLE II

SOUND PRESSURE HARMONIC LEVELS MEASURED AT THE DUCT WALL AND WITH BOOM MICROPHONES DURING REFERENCE-DUCT TESTS

(a) Reference Duct No. 1; 6000 rpm

Tabulation of Harmonic Sound Pressure Levels (dB re 2 x 10^{-4} μbar)								
Harmonic Frequency (Hz)	Duct Wall Transducers			Boom Microphones B2 and B3*				
				Azimuth Angle (η)				
	K1	K2	K3	20	50	80	110	140
300	137	143	122	71 75	67 73	65 71	67 73	72 75
600	127	135	107	73 78	75 85	73 80	70 77	78 82
900	117	126	107	71 77	73 80	67 74	67 72	67 77
1200	109	124	106	71 76	72 78	70 76	67 75	72 78
1500	106	113	105	66 71	69 76	70 75	70 75	72 79

*Upper values are B2 measurements (10-ft radius)
Lower values are B3 measurements (5-ft radius)

TABLE II Continued

(b) Reference Duct No. 1; 8000 rpm

Tabulation of Harmonic Sound Pressure Levels (dB re 2 x 10^{-4} μbar)								
Harmonic Frequency (Hz)	Duct Wall Transducers			Boom Microphones B2 and B3* Azimuth Angle (η)				
	K1	K2	K3	20	50	80	110	140
400	142	148	130.5	80 83	78 89	73 82	80 89	76 87
800	133.5	141	116	82 90	85 92	78 85	81 85	80 87
1200	125.5	132	121	80 87	87 92	87 91	80 88	80 88
1600	117	129	112	81 88	81 87	76 82	76 84	80 88
2000	113	-	114	80 85	83 88	75 80	78 83	79 90

*Upper values are B2 measurements (10-ft radius)
Lower values are B3 measurements (5-ft radius)

TABLE II CONCLUDED

(c) Reference Duct No. 2; 8000 rpm

Tabulation of Harmonic Sound Pressure Levels (dB re 2×10^{-4} μ bar)								
Harmonic Frequency (Hz)	Duct Wall Transducers			Boom Microphones B2 and B3 * Azimuth Angle (η)				
	K1	K2	K3	10	40	70	100	130
400	128.5	134.5	145	80 91	82 87	78 84	80 84	77 89
800	111	120	137	79 88	78 82	73 81	78 82	79 86
1200	114	112	128	80 89	81 88	78 83	76 82	83 86
1600	115	113	120	81 90	82 90	81 85	77 82	84 88
2000	112	113	115	81 88	84 93	79 85	77 83	84 87

*Upper values are B2 measurements (10-ft radius)
Lower values are B3 measurements (5-ft radius)

TABLE III

COMPARISON OF MEASURED AND ESTIMATED
RESONATOR RESONANCE FREQUENCIES IN PROPELLER DUCT

Orifice Size		Duct Field		Resonance Frequency (Hz)		
d (in.)	t (in.)	SPL (dB)	U_c (fps)	f_m	$fe^{(1)}$	$fe^{(2)}$
0.625	0.125	119	37	540	545	607
		130	52	535	545	607
		141	79	550	545	607
0.625	0.125	131	69	930	890	992
		140	88	885	890	992
0.375	0.187	121	50	560	580	609
		131	65	580	580	609
		142	83	590	580	609

U_c = measured cross flow velocity.

f_m = frequency at maximum gain measurement.

fe = estimated resonance frequency, using

$^{(1)}\ell_e = t + 0.85\ d$ and $^{(2)}\ell_e = t + 0.85\ d\ (1-0.625\ d/d_c)$

TABLE IV

CHANGE IN HARMONIC SOUND PRESSURE LEVELS (dB) DUE TO INSTALLATION OF A UNIFORM ARRAY OF RESONATORS (RELATIVE TO REFERENCE-DUCT MEASUREMENTS)

(a) Modified Duct No. 1; 8000 rpm

Resonator Frequency = 400 Hz; d = 0.375 in., t = 0.187 in.								
Frequency (Hz)	K1	K3	Boom Location (η)					Resonator Gain (dB)
			20°	50°	80°	110°	140°	
400	2	-1	-1	-2	1	6	6	3
800	1	1	2	0	0	-1	1	-2
1200	1	1	0	-1	-1	1	1	-12
1600	6	-1	0	-1	0	-3	2	-10

Resonator Frequency = 800 Hz; d = 0.375 in., t = 0.187 in.								
Frequency (Hz)	K1	K3	Boom Location (η)					Resonator Gain (dB)
			20°	50°	80°	110°	140°	
400	1.5	-1	2	0	1	1	1	1
800	1.5	1	2	1	-1	2	3	7
1200	2	1	2	3	1	3	1	3
1600	4	1	2	5	2	1	4	-1

Resonator Frequency = 800 Hz; d = 0.625 in., t = 0.125 in.								
Frequency (Hz)	K1	K3	Boom Location (η)					Resonator Gain (dB)
			20°	50°	80°	110°	140°	
400	3	0	2	-4	5	4	2	0
800	3	2	8	9	7	6	9	10
1200	-2	-4	7	0	-4	-3	3	5
1600	7	3	0	3	-1	2	7	0

TABLE IV Continued

(b) Modified Duct No. 1; 6000 rpm

Resonator Frequency = 600 Hz; d = 0.375 in., t = 0.187 in.								
Frequency (Hz)	K1	K3	Boom Location (η)					Resonator Gain (dB)
			20°	50°	80°	110°	140°	
300	0	0		1			3	2
600	1	0		1			4	8
900	1	1		6			9	3
1200	3	1		3			5	0

Resonator Frequency = 600 Hz; d = 0.625 in., t = 0.125 in.								
Frequency (Hz)	K1	K3	Boom Location (η)					Resonator Gain (dB)
			20°	50°	80°	110°	140°	
300	2	0		4			3	1
600	3	1		6			5	11
900	3	2		9			11	1
1200	4	2		5			1	-6

Resonator Frequency = 900 Hz; d = 0.625 in., t = 0.125 in.								
Frequency (Hz)	K1	K3	Boom Location (η)					Resonator Gain (dB)
			20°	50°	80°	110°	140°	
300	0	0		1			3	-3
600	1	0		1			4	0
900	1	1		6			9	8
1200	3	1		3			5	1

TABLE IV Concluded

(c) Modified Duct No. 2; 8000 rpm

Resonator Frequency = 400 Hz; d = 0.375 in., t = 0.187 in.									
Frequency (Hz)	K1	K2	K3	Boom Location (η) 10°	40°	70°	100°	130°	Resonator Gain (dB)
400	3	1	1	2	3	1	-1	2	3.5
800	3	0	1	3	7	5	1	-1	0
1200	2	3	1	1	2	0	-1	-2	-3
1600	3	2	0	3	5	6	1	-1	-5

Resonator Frequency = 800 Hz; d = 0.375 in., t = 0.187 in.									
Frequency (Hz)	K1	K2	K3	Boom Location (η) 10°	40°	70°	100°	130°	Resonator Gain (dB)
400	1	2	1	-1	0	2	1	1	-2
800	3	1	2	1	9	6	4	4	3
1200	2	0	0	0	3	2	1	-1	0
1600	4	3	3	2	6	3	1	4	-6

Resonator Frequency = 800 Hz; d = 0.625 in., t = 0.125 in.									
Frequency (Hz)	K1	K2	K3	Boom Location (η) 10°	40°	70°	100°	130°	Resonator Gain (dB)
400	-2	0	0	4	2	-4	-1	3	-1
800	9	0	0	10	13	11	5	5	26
1200	0	3	2	2	2	-1	3	-3	-2
1600	2	2	2	3	4	0	1	2	-1

TABLE V

CHANGE IN HARMONIC SOUND PRESSURE
LEVELS (dB) DUE TO STAGGERED ARRAYS OF RESONATORS

MODIFIED DUCT NO. 1; 8000 rpm

Staggered Array of Resonators							
Frequency			Boom Location (η)				
(Hz)	K1	K3	20°	50°	80°	110°	140°
400	1	0	2	-3	3	6	7
800	-3	7	2	2	11	1	5
1200	0	3	4	-4	-6	1	4
1600	0	3	-1	-1	0	2	0

Assymetric Array of Resonators							
Frequency			Boom Location (η)				
(Hz)	K1	K3	20°	50°	80°	110°	140°
400	2	-1	0	-2	7	5	0
800	3	12	7	6	10	6	8
1200	3	1	8	1	-7	2	3
1600	17	7	4	5	-1	3	1

Staggered Array with Absorptive Cavity							
Frequency			Boom Location (η)				
(Hz)	K1	K3	20°	50°	80°	110°	140°
400	2	0	3	-3	4	6	8
800	-3	6	3	4	11	0	7
1200	-5	10	7	5	4	1	8
1600	8	-1	6	5	3	2	3

TABLE VI

HARMONIC SOUND PRESSURE LEVELS, WITH UNIFORM ARRAYS OF RESONATORS TUNED TO VARIOUS FREQUENCIES

(a) Test Results with 0.625-in. Diameter, 0.125-in. Thick Orifice

Resonator Array	Harmonic	K1 (dB)	Res ① Gain (dB)	K2 (dB)	Res ② Gain (dB)	K3 (dB)	Res ③ Gain (dB)	K4 (dB)	Res ④ Gain (dB)	B_1 L/E at ℄ (dB)	B_3 $\eta=40°$ (dB)	TL (Wall) (dB)
Reference	1	128.5	(2)	134.5	(2)	145	(2)	149	(2)	108	87	16.5
Solid Wall	2	112	(2)	119	(2)	136.5	(2)	140	(2)	99	82	24.5
Duct	3	114	(2)	112	(2)	127.5	(2)	138	(2)	108	88	13.5
d_o = 0.625 in., t = 0.125 in.	1	130	+.5	136.5	+3	145.5	(1)	151.5	(2)	114	87	15.5
	2	112	0	117	+2	137.5	(1)	140	(2)	107	88	25.5
f_r = 600 Hz	3	119	-4	116	-10	129	(1)	140.5	(2)	107	89	10
d_o = 0.625 in., t = 0.125 in.	1	127	+1.5	135	+1	148	-4	150	(2)	113	89	21
(3) f_r = 700 Hz	2	114	+9N	119	+12	140.5	0	141	(2)	103	90	26.5
f_r = 1050 Hz	3	110	-4N	110	-4	133.5	+6.5	140	(2)	110	89	23.5
d_o = 0.625 in., t = 0.125 in.	1	126	0	135	-.5	145	-0.5	152	(2)	110	89	19
	2	120	+26	120	+26	137	+16	139	(2)	114	95	17
f_r = 800 Hz	3	114	0	115	-2	127	0	141	(2)	108	90	13
d_o = 0.625 in., t = 0.125 in.	1	126	0	134.5	-1.5	146	-1.0	151.5	(2)	108	84	20
	2	122	+25	122	+23	137	+16	138	(2)	114	95	15
f_r = 870 Hz	3	113	0	112	+1	127	0	140.5	(2)	106	89	14
d_o = 0.625 in., t = 0.125 in.	1	127	-1	135	-1	146	-12	151	(2)	109	88	19
	2	121	+10	125	+6	136	-4	142	(2)	104	91	15
f_r = 1050 Hz	3	113N	N	113N	N	129	+1	141	(2)	107	92	16

NOTE: Symbols are explained in listing following Table VI (c)

TABLE VI Concluded

(b) Test Results with 0.375-in. Diameter Tapered Orifice (approximate orifice thickness = 0.010 in.), with the Frequency Tuned Experimentally

Resonator Array	rpm	Harmonic	K1 (dB)	Res ① Gain (dB)	K2 (dB)	Res ② Gain (dB)	K3 (dB)	Res ③ Gain (dB)	K4 (dB)	Res ④ Gain (dB)	B1 at ℄ (dB)	B3 η=40° (dB)	TL (Wall) (dB)
		1	128.5		134.5		145		149		108	87	16.5
Reference	8000	2	112		119		136.5		140		99	82	24.5
		3	114		112		127.5		138		108	88	13.5
		1	130	-2.0	135	+3.5	144.5	(2)	151	(2)	107	88	14.5
d_o = 0.375 in., t = 0.010 in.	8000	2	110	+5.0	118	-1.0	134.5	(2)	140	(2)	103	85	24.5
f_r = 520 Hz		3	112	-6.0	113	0	127	(2)	141	(2)	109	94	15
		1	127.5	-0.5	135.5	0	145	(2)	150.5	(2)	110	91	17.5
d_o = 0.375 in., t = 0.010 in.	8000	2	116	+6.0	121	+12	136	(2)	142	(2)	98	87	20
f_r = 930 Hz		3	116	-4.0	113	+4.0	128	(2)	140	(2)	114	93	12
		1	128.5	(1)	136	-2.5	145	(2)	151.5	(2)	(1)	88	16.5
d_o = 0.375 in., t = 0.010 in.	8000	2	111	(1)	120	+1.0	136	(2)	140	(2)	(1)	83	25
f_r = 650 Hz		3	116	(1)	118	-1.5	124	(2)	140.5	(2)	(1)	90	8.0

(c) Test Results with 0.375-in. diameter, 0.187-in. thick orifice

		1	131.5	+0.5	135.5	+3.5	146	(1)	150	(2)	108	90	14.5
d_o = 0.375 in., t = 0.187 in.	8000	2	115	-2.0	119	0	137	(1)	140	(2)	101	89	22
f_r = 400 Hz		3	116	-7.0	115	-3.0	128	(1)	139	(2)	108	90	12
		1	129	+7.0	137	+2.5	147	+1.0	150	(2)	108	87	18
d_o = 0.375 in., t = 0.187 in.	8000	2	115	+6.0	121	-5.0	137	-6.0	141	(2)	104	84	22
f_r = 330 Hz		3	117	+1.0	115	-5.5	129	-14	140	(2)	108	90	12

TL (dB) – the difference in harmonic level between K3 and K1

Resonator Gain (dB) – the gain measured between K at duct wall and $K^{(r)}$ in adjacent resonator cavity

B1 is measured at the duct center line

(1) Levels not recorded

(2) Resonator omitted from this row

(3) First two rows of resonators tuned to the lower frequency

N Indicates that sound field consisted mainly of noise

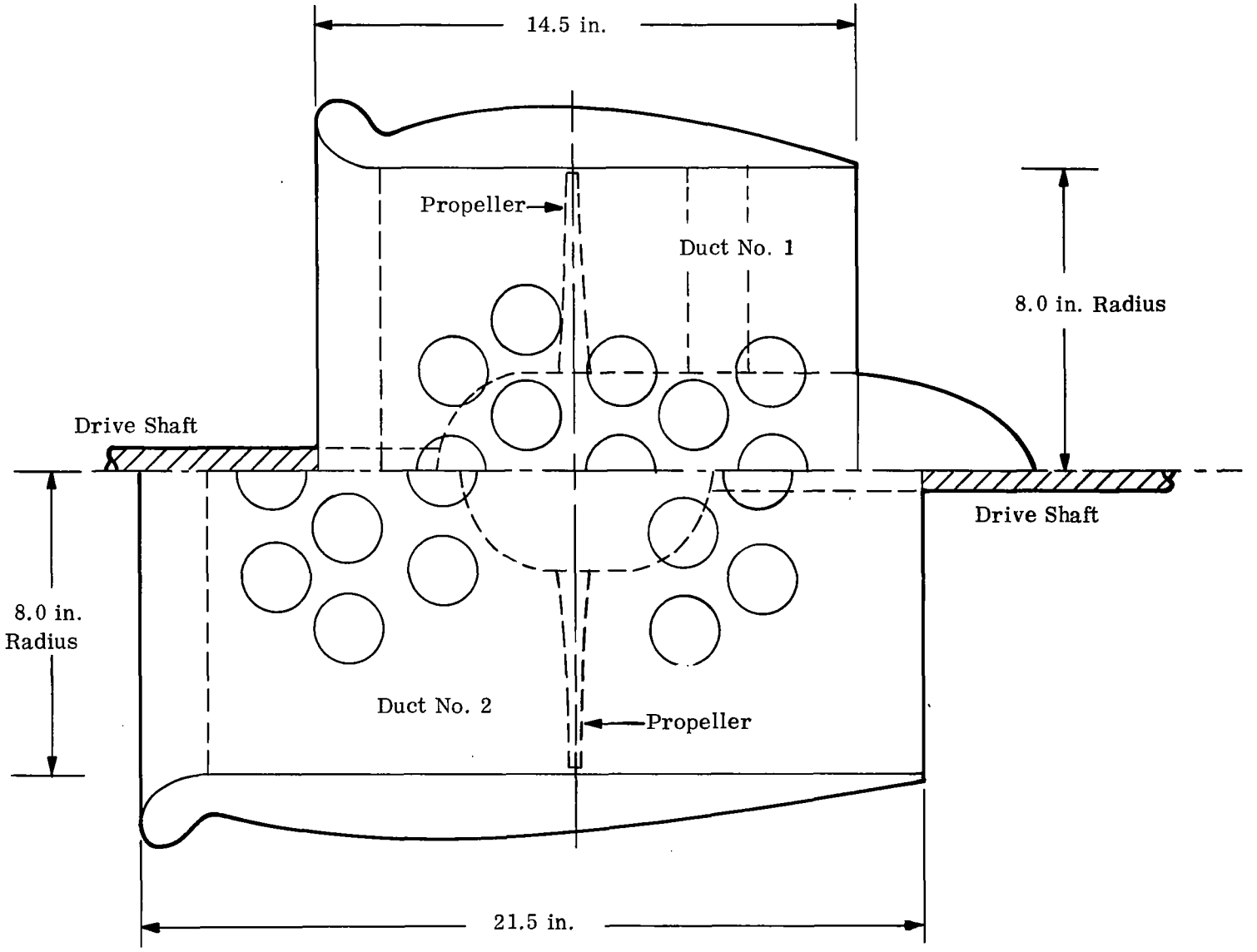

Figure 1. Basic Geometry of Model Propeller Ducts

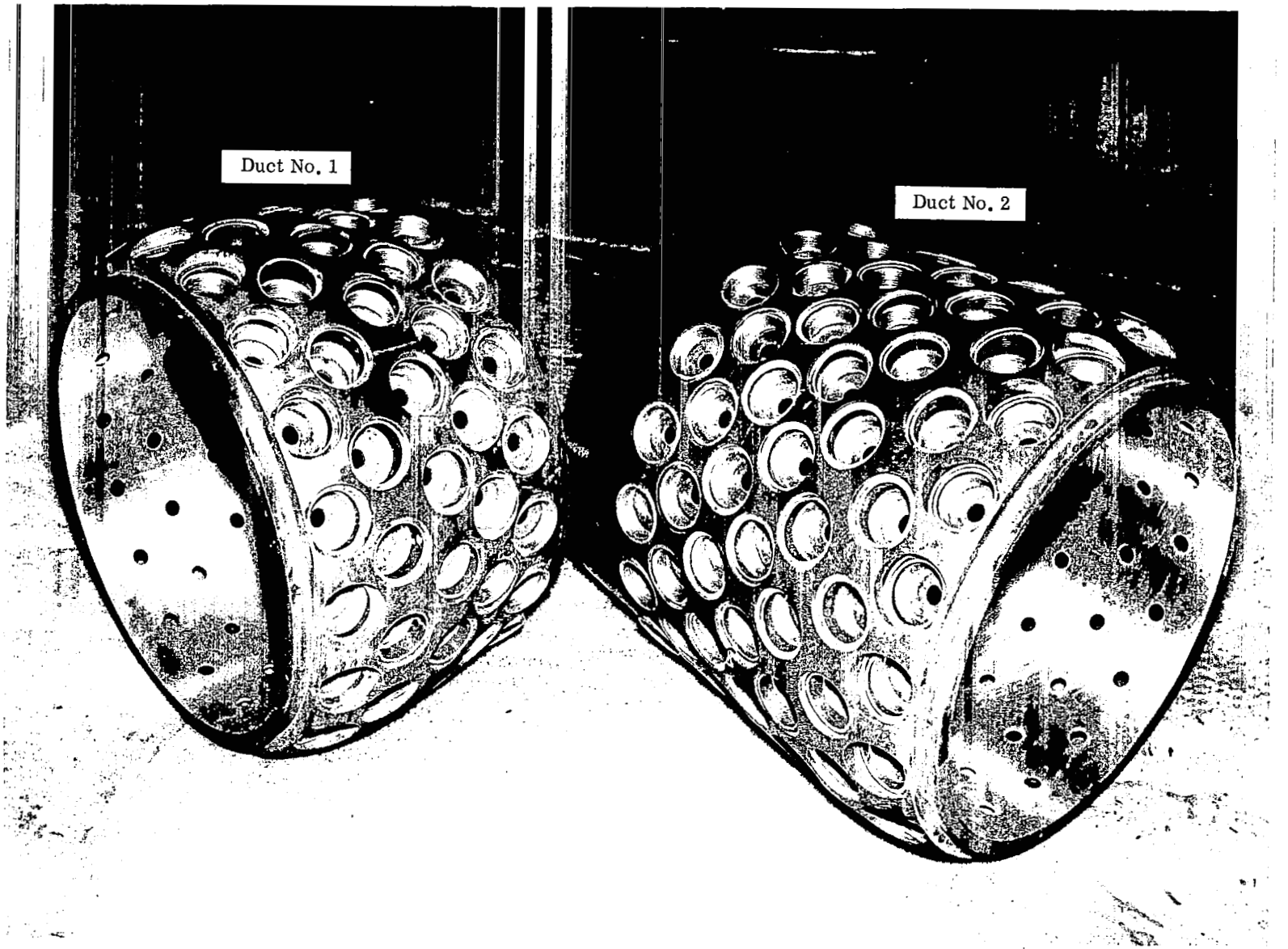

Figure 2. Model Propeller Ducts, Modified For Resonator Installation

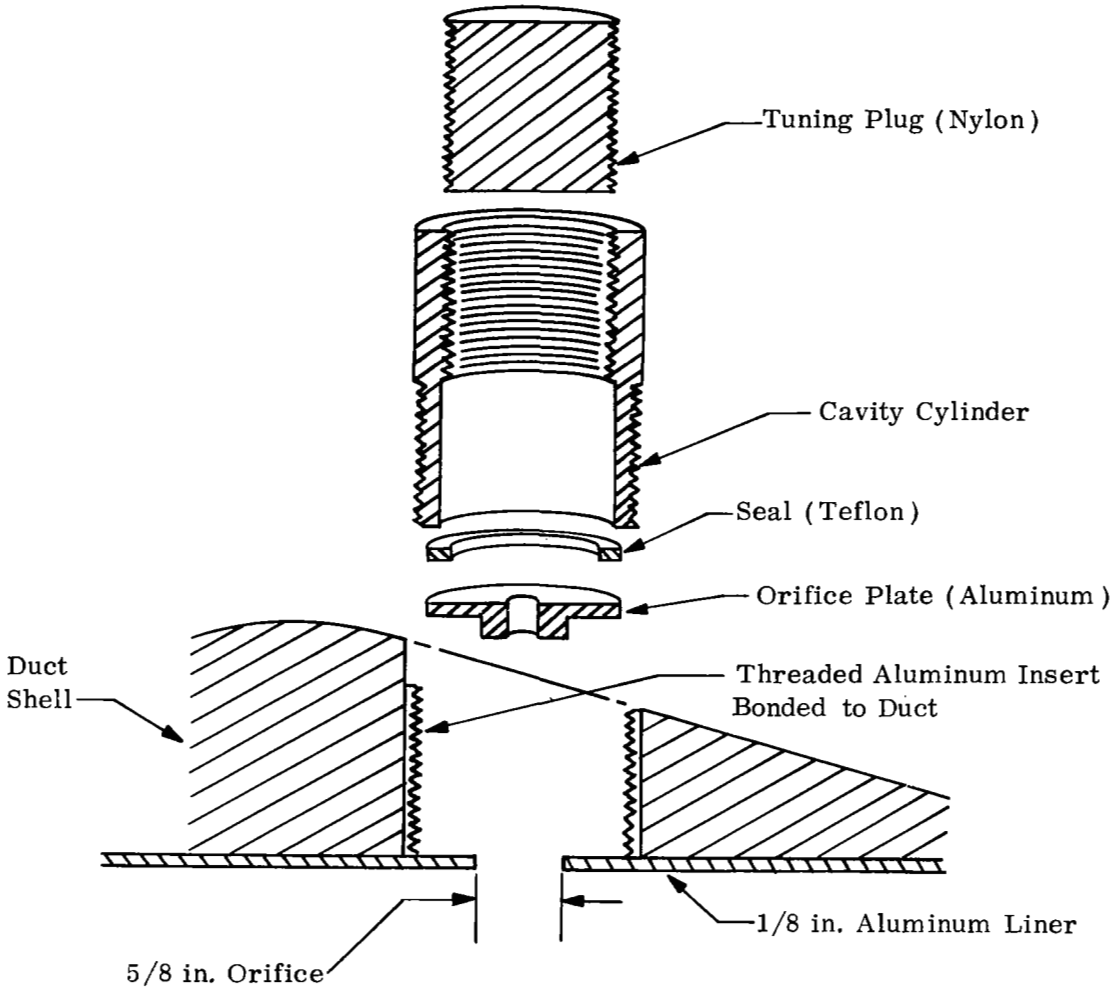

Figure 3. Details of Duct Modification and Basic Resonator Design

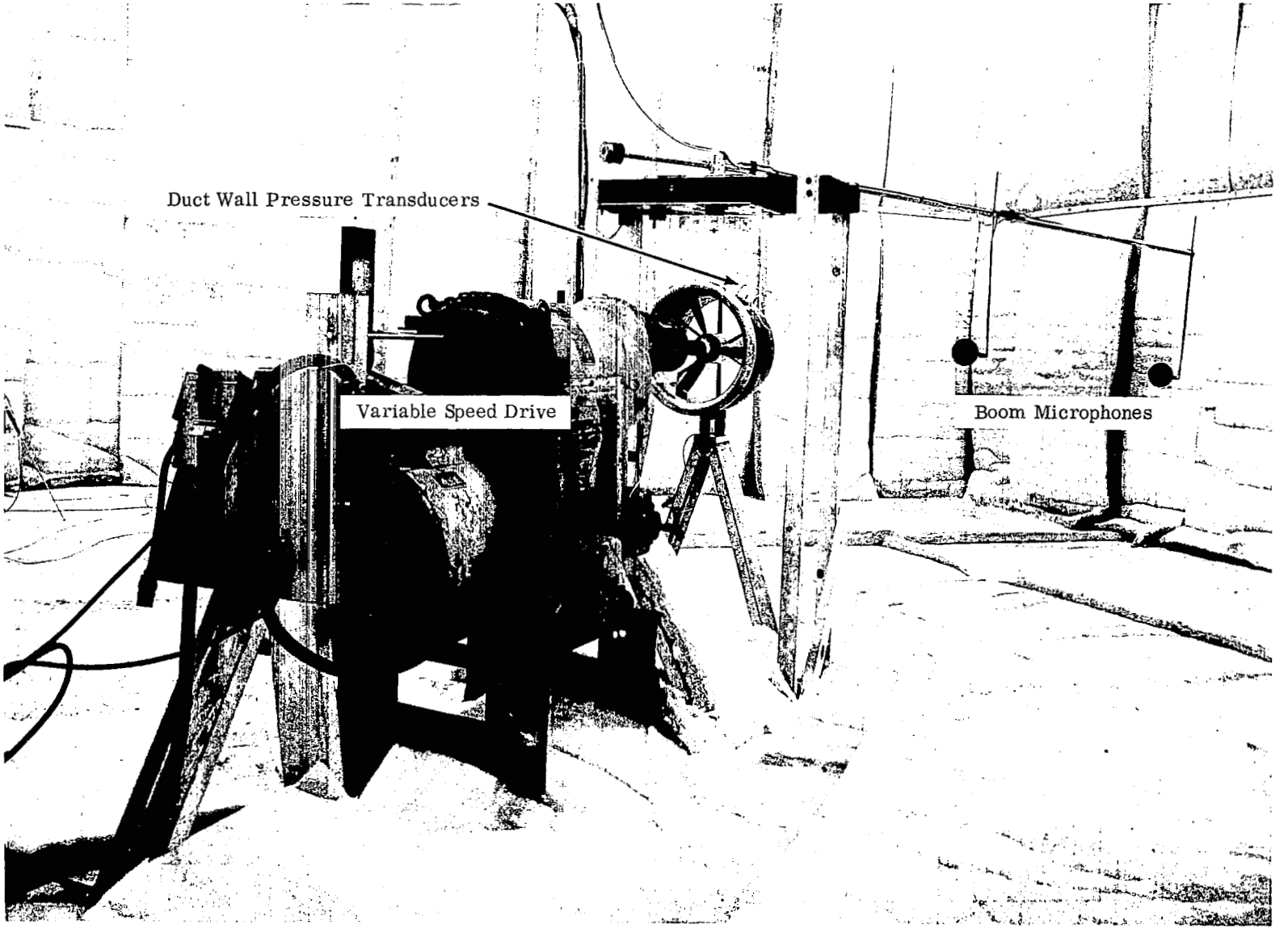

Figure 4. Model Ducted-Propeller System In-Test Facility

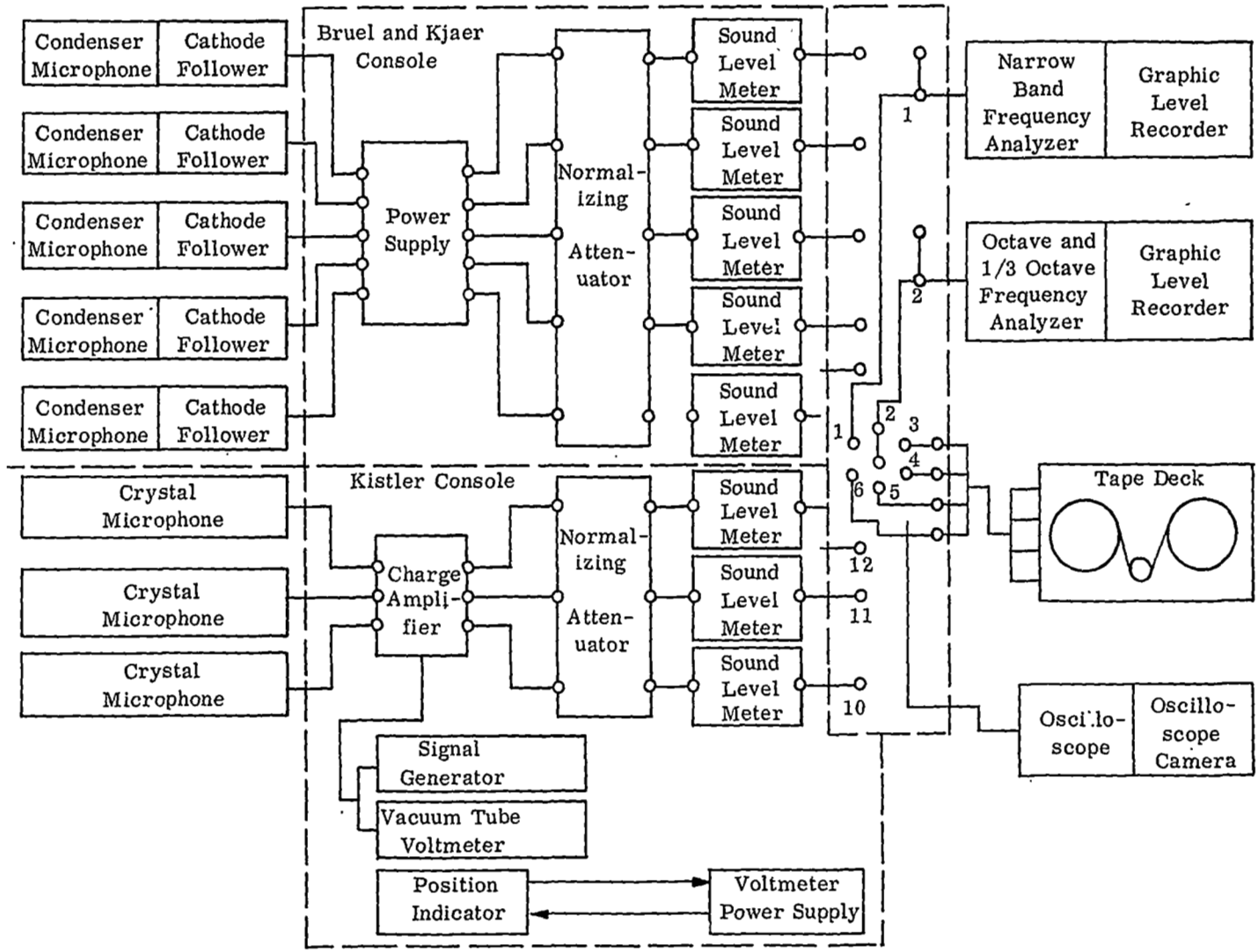

Figure 5. Acoustic Instrumentation for Model Ducted-Propeller Study

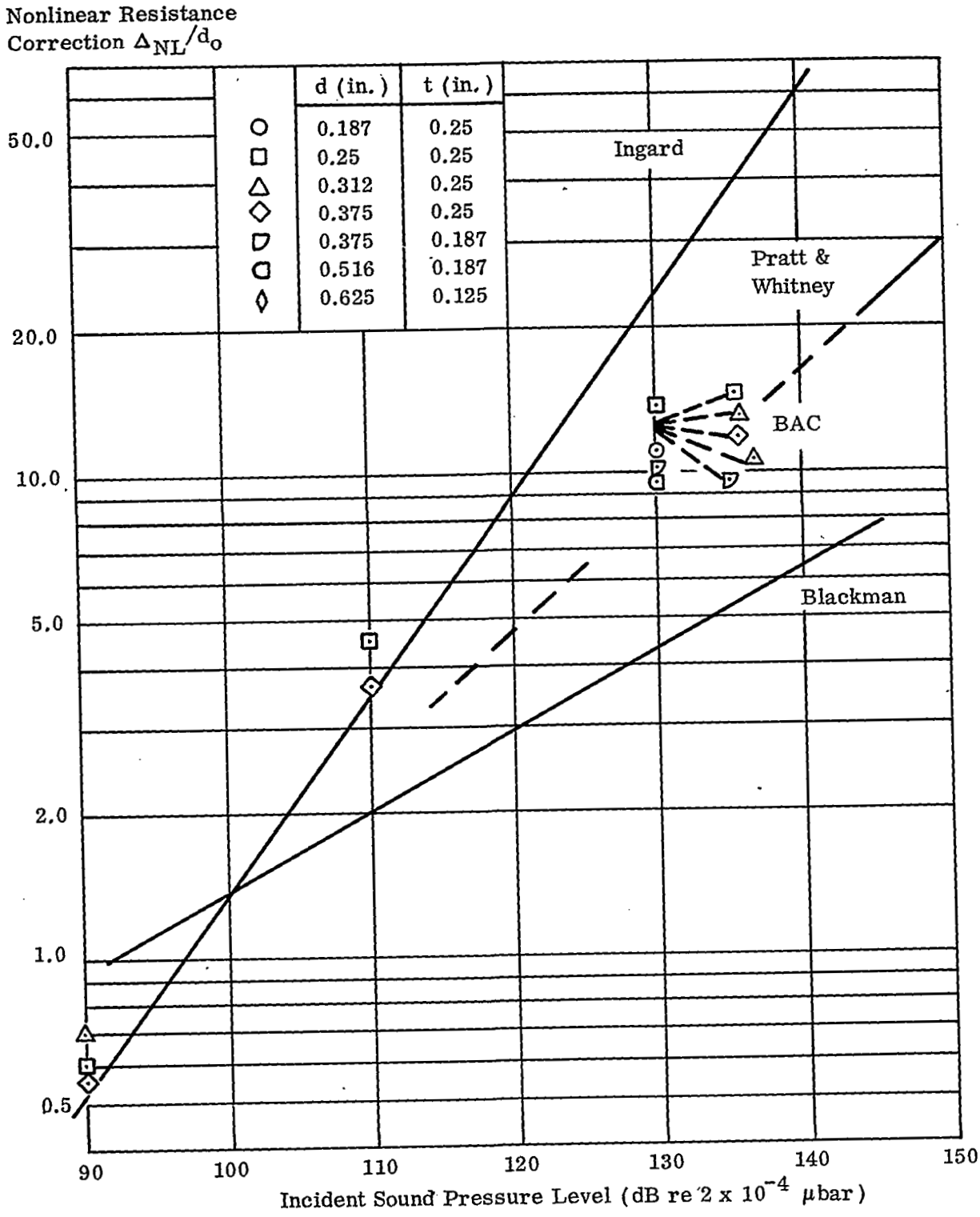

Figure 6. Impedance-Tube Evaluation of Resonator Nonlinear Resistance Correction

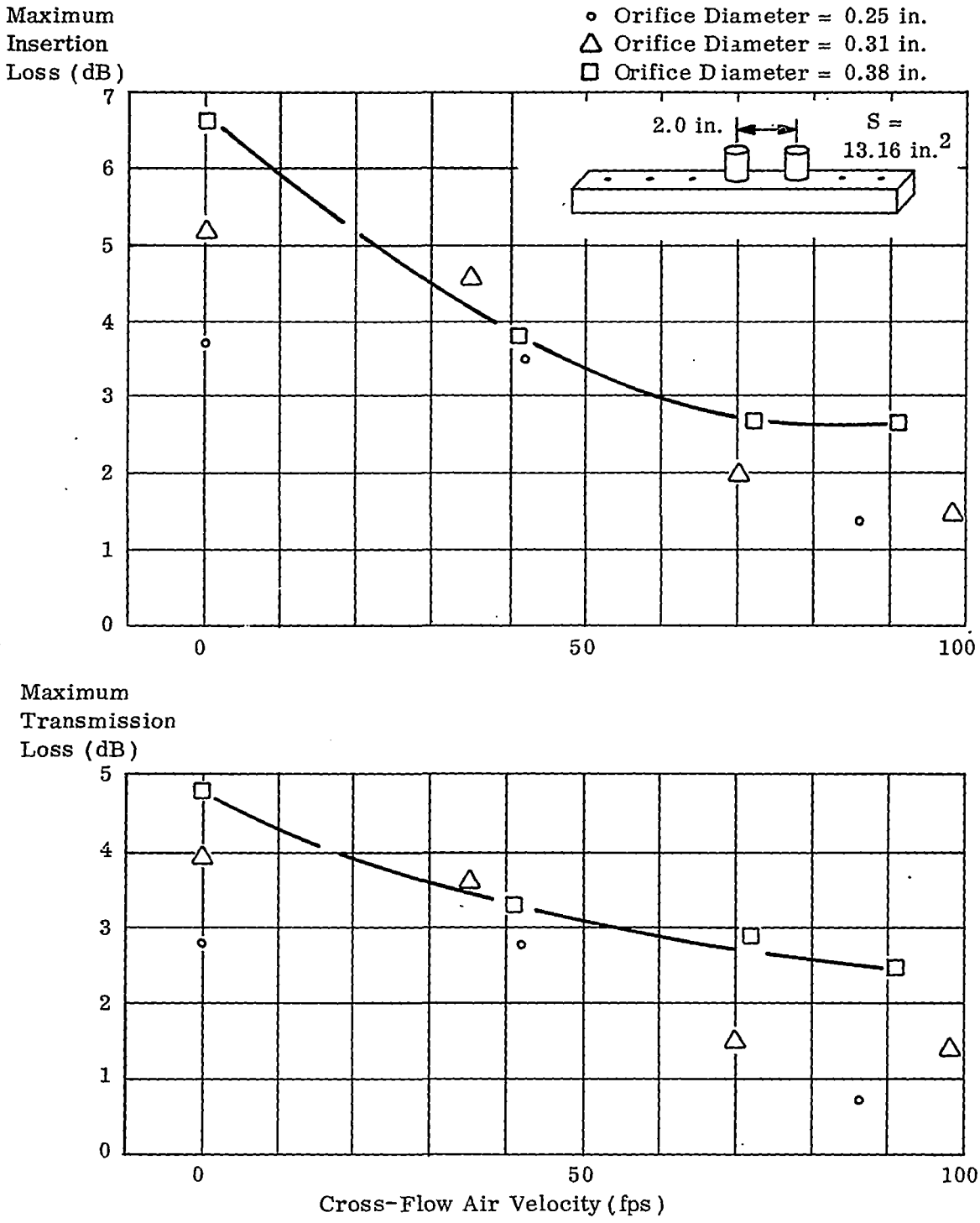

Figure 7. Sidebranch Resonator Effect in Plane-Wave Tube with Air Flow

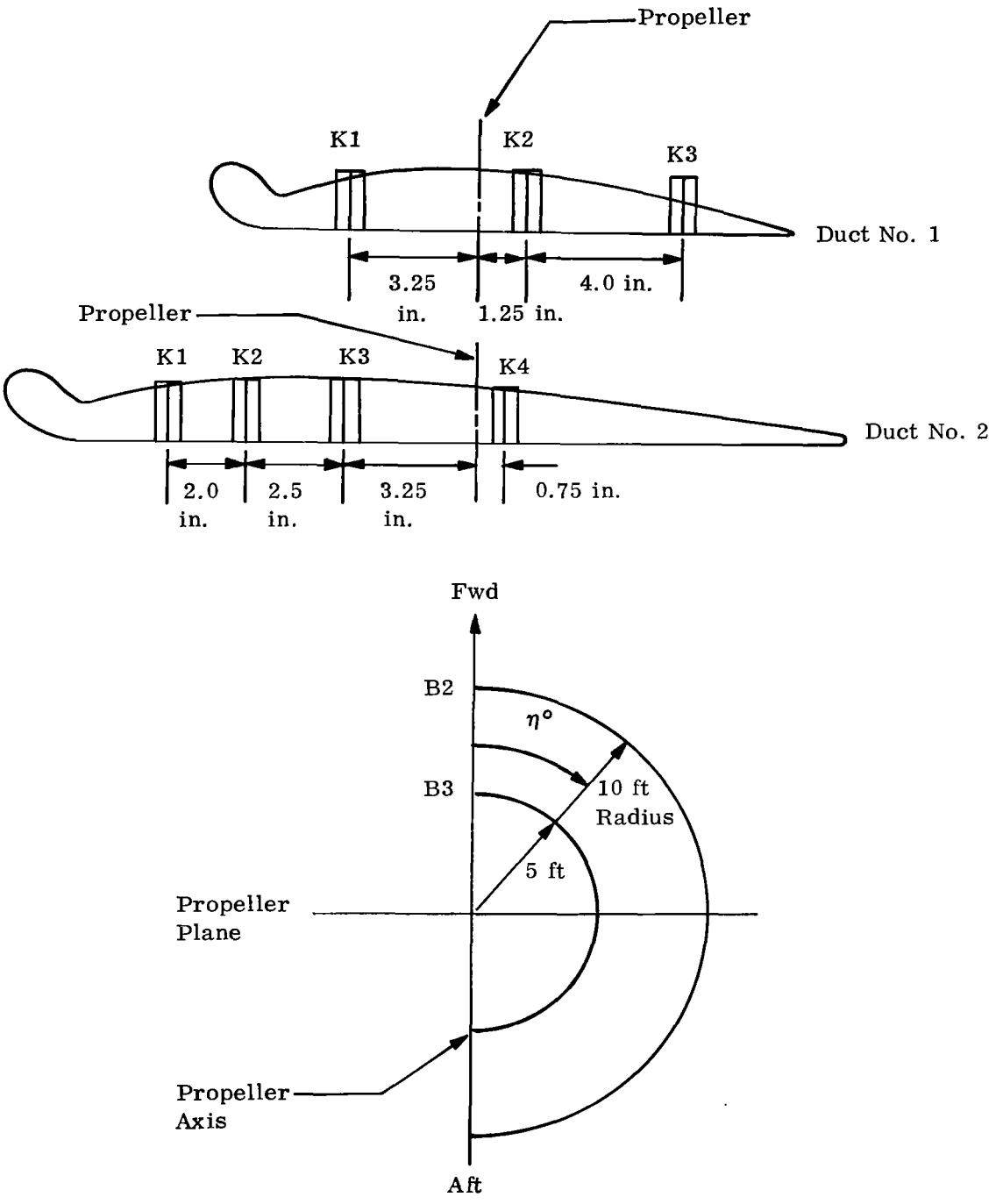

Figure 8. Location and Nomenclature of Microphones for Sound Surveys

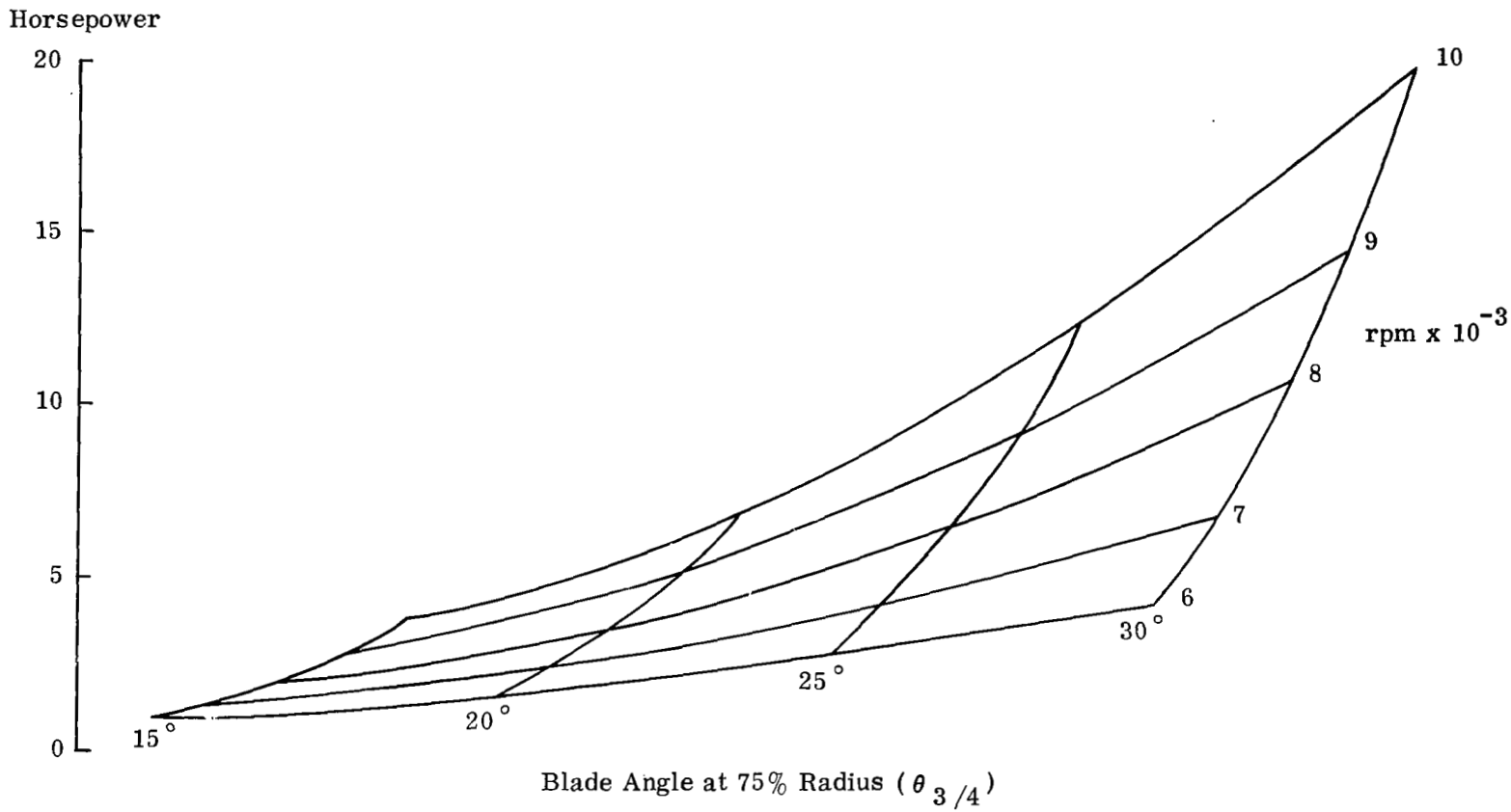

Figure 9. Theoretical Performance Range of Model Ducted-Propeller System

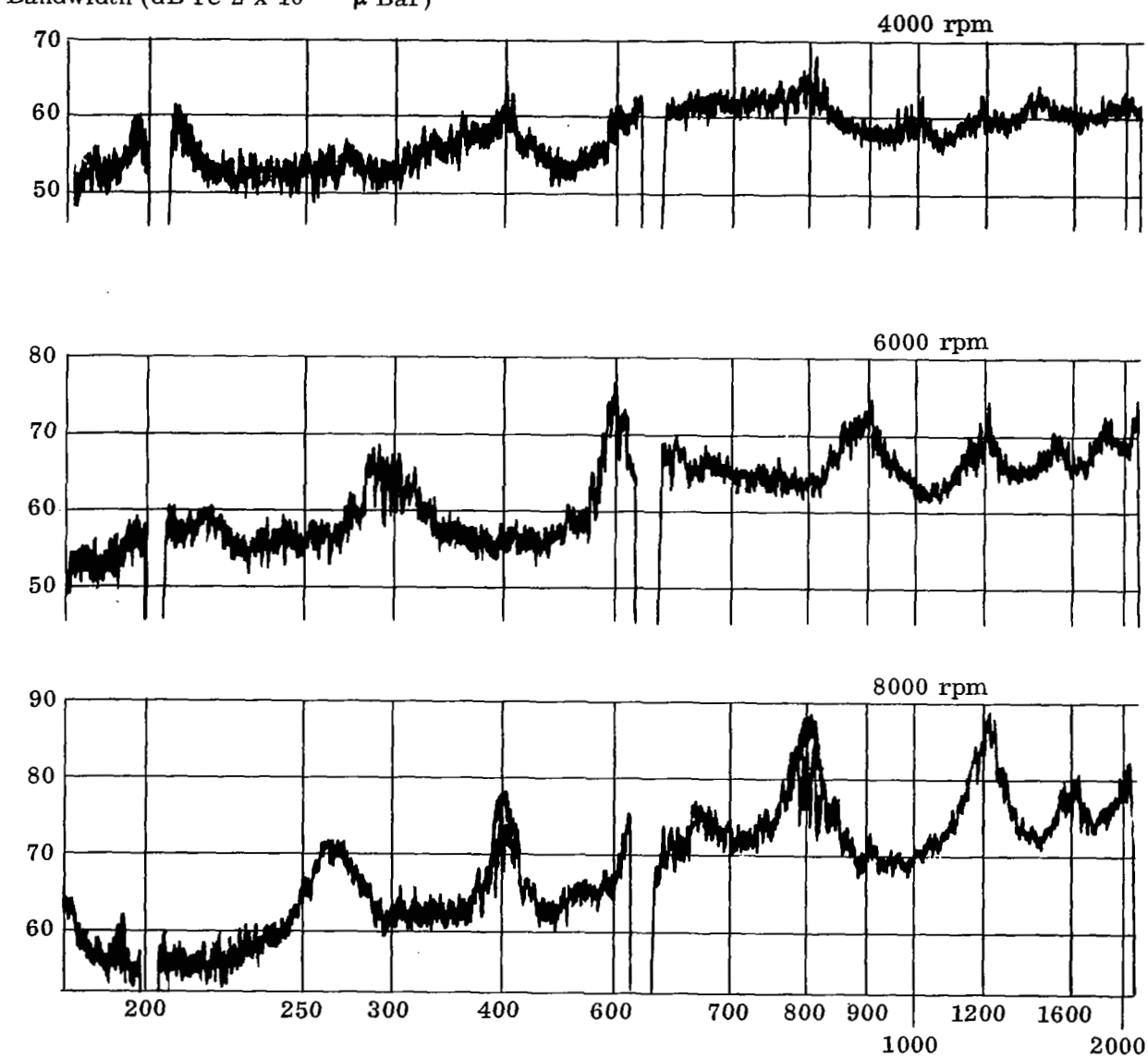

Figure 10. Sound Pressure Spectra at Boom Microphone B2, for Propeller Speeds of 4000, 6000, and 8000 rpm in Reference Duct No. 1

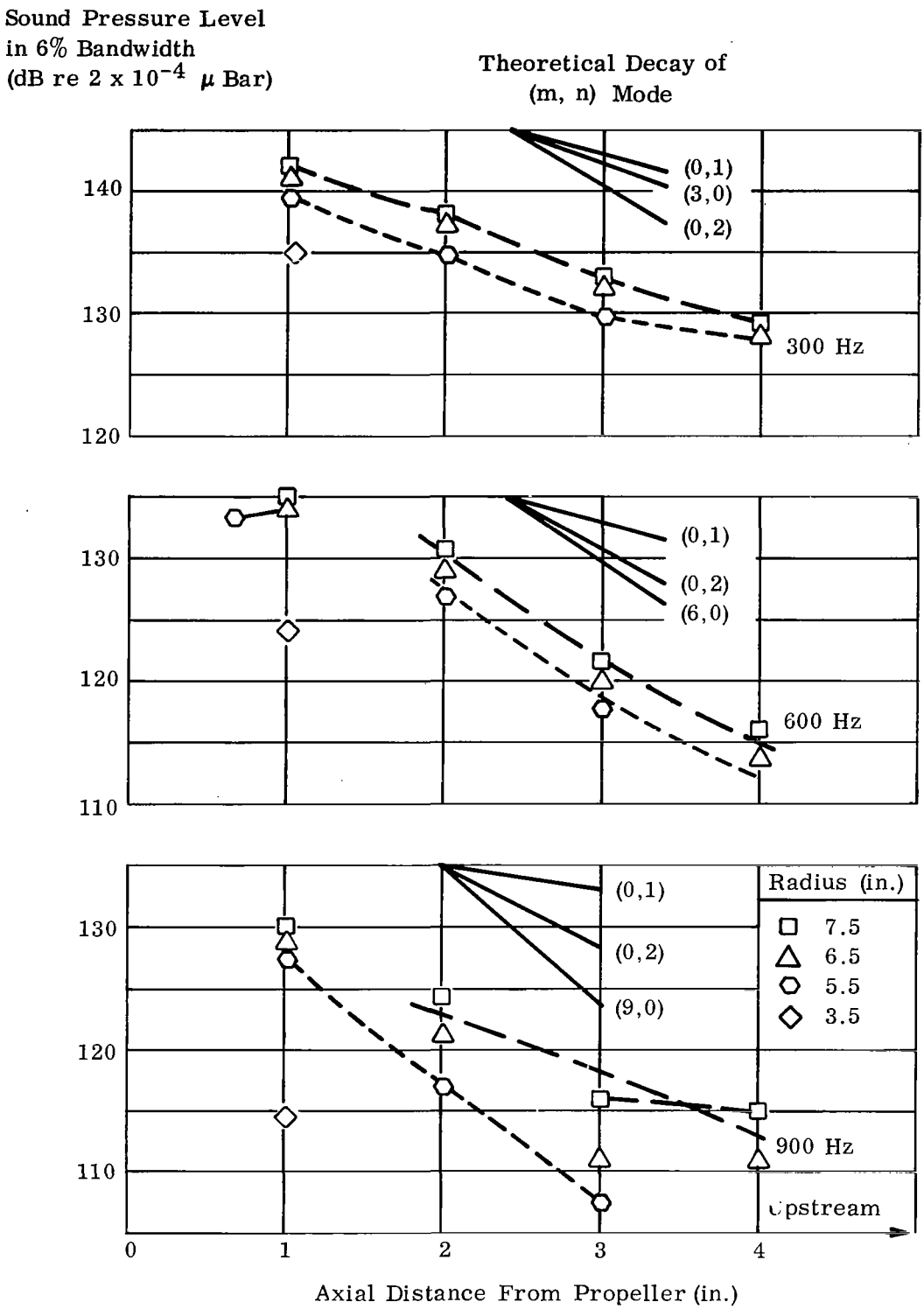

Figure 11 (a). Spatial Distribution of Harmonic Sound Levels in Duct No. 1 for 6000 rpm Propeller Speed

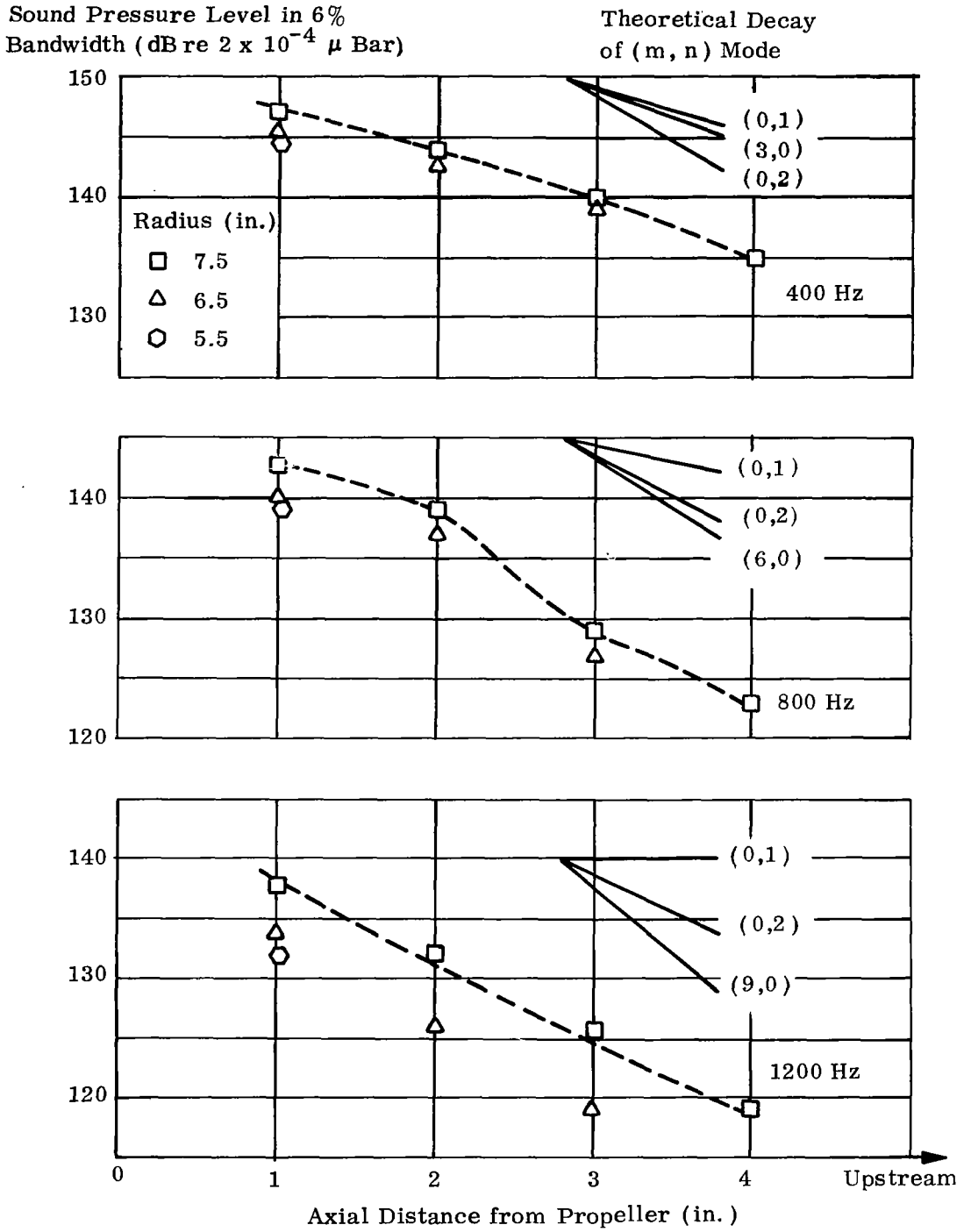

Figure 11 (b). Spatial Distribution of Harmonic Sound Levels in Duct No. 1 for 8000 rpm Propeller Speed

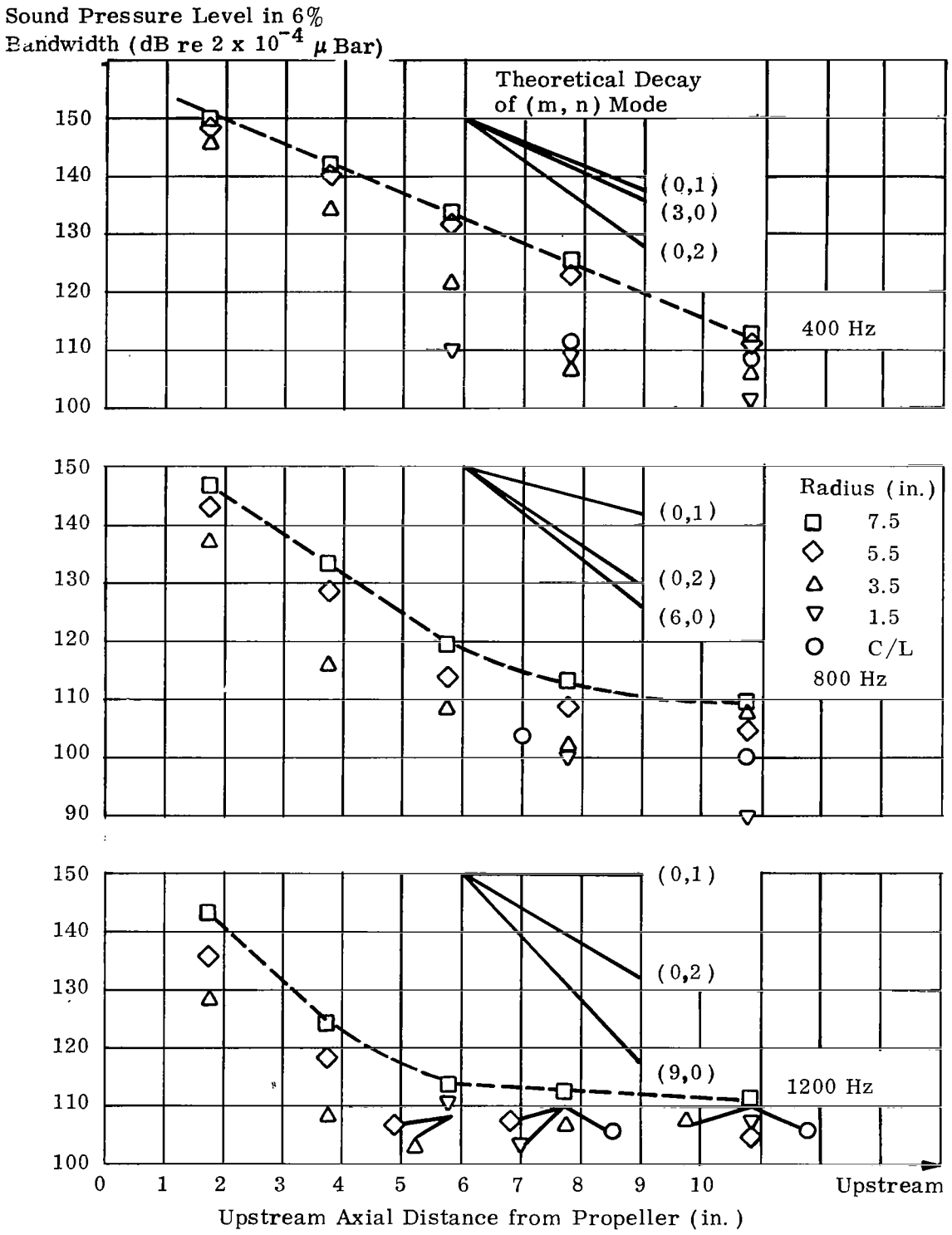

Figure 12. Spatial Distribution of Harmonic Sound Levels in Duct No. 2 for 8000 rpm Propeller Speed

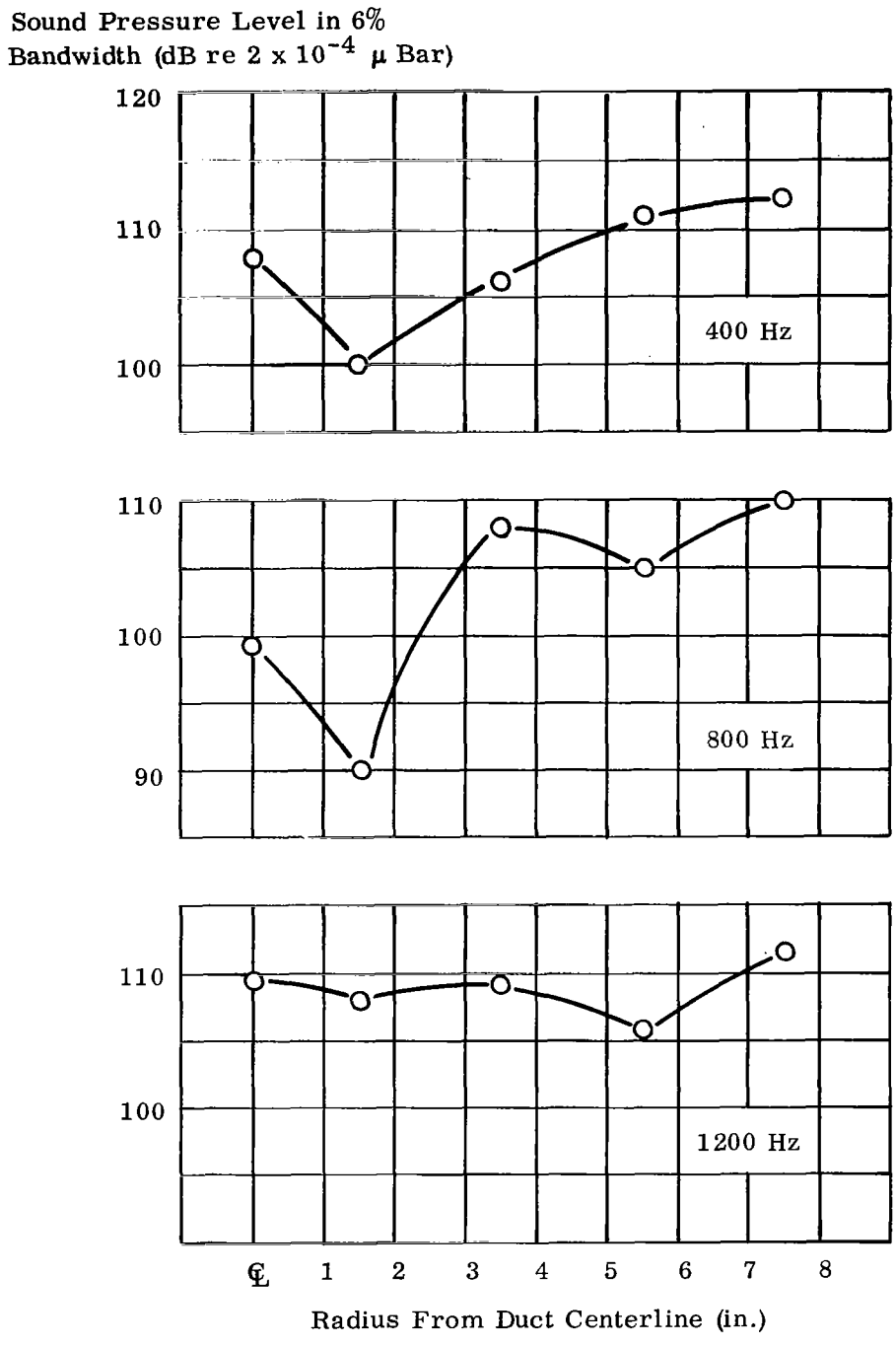

Figure 13. (a). Radial Distribution of Sound Level in Duct No. 2 at 8000 rpm (Axial location: 10.75 in. from Propeller)

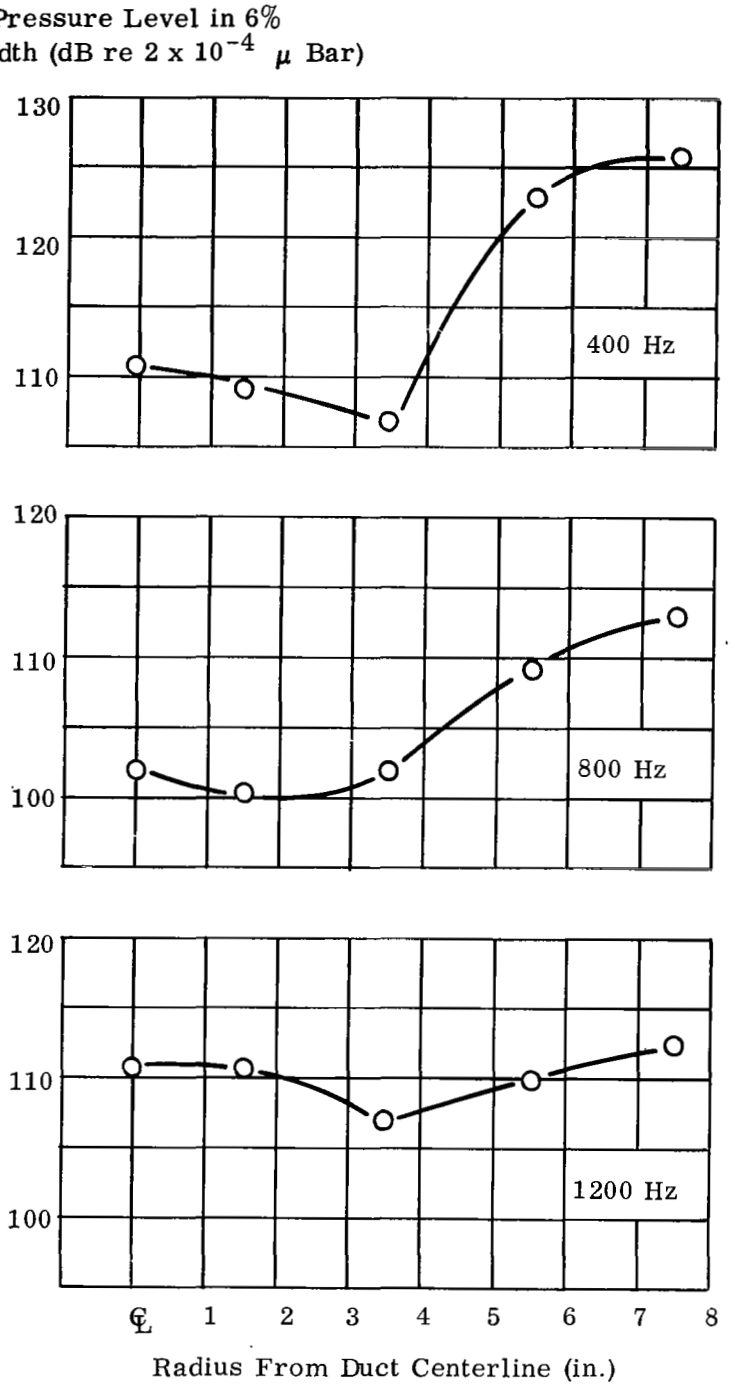

Figure 13. (b). Radial Distribution of Sound Level in Duct No. 2 at 8000 rpm (Axial Location: 7.75 in. from Propeller)

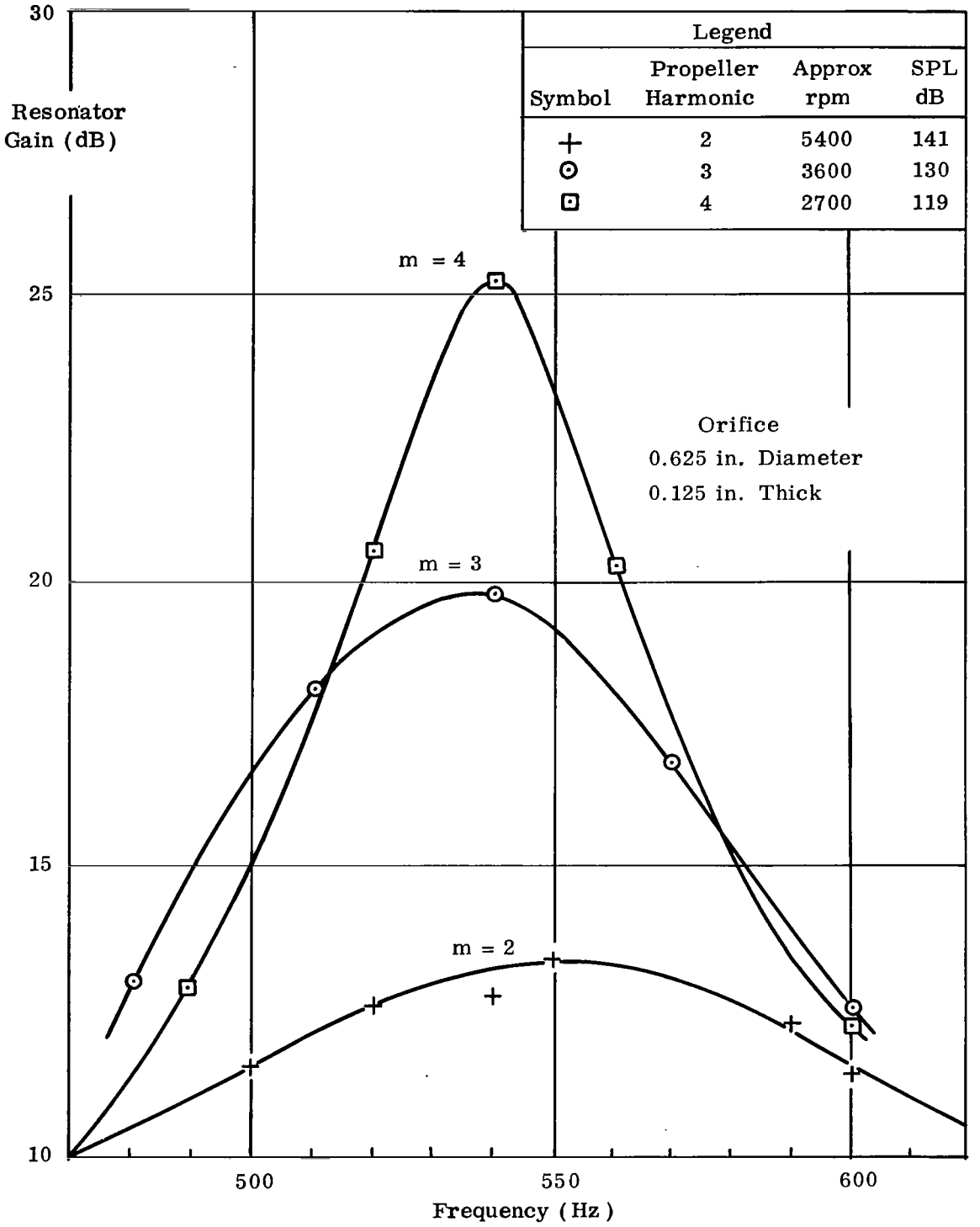

Figure 14. Measured Gain in Sound Pressure between Resonator Cavity and Duct Wall

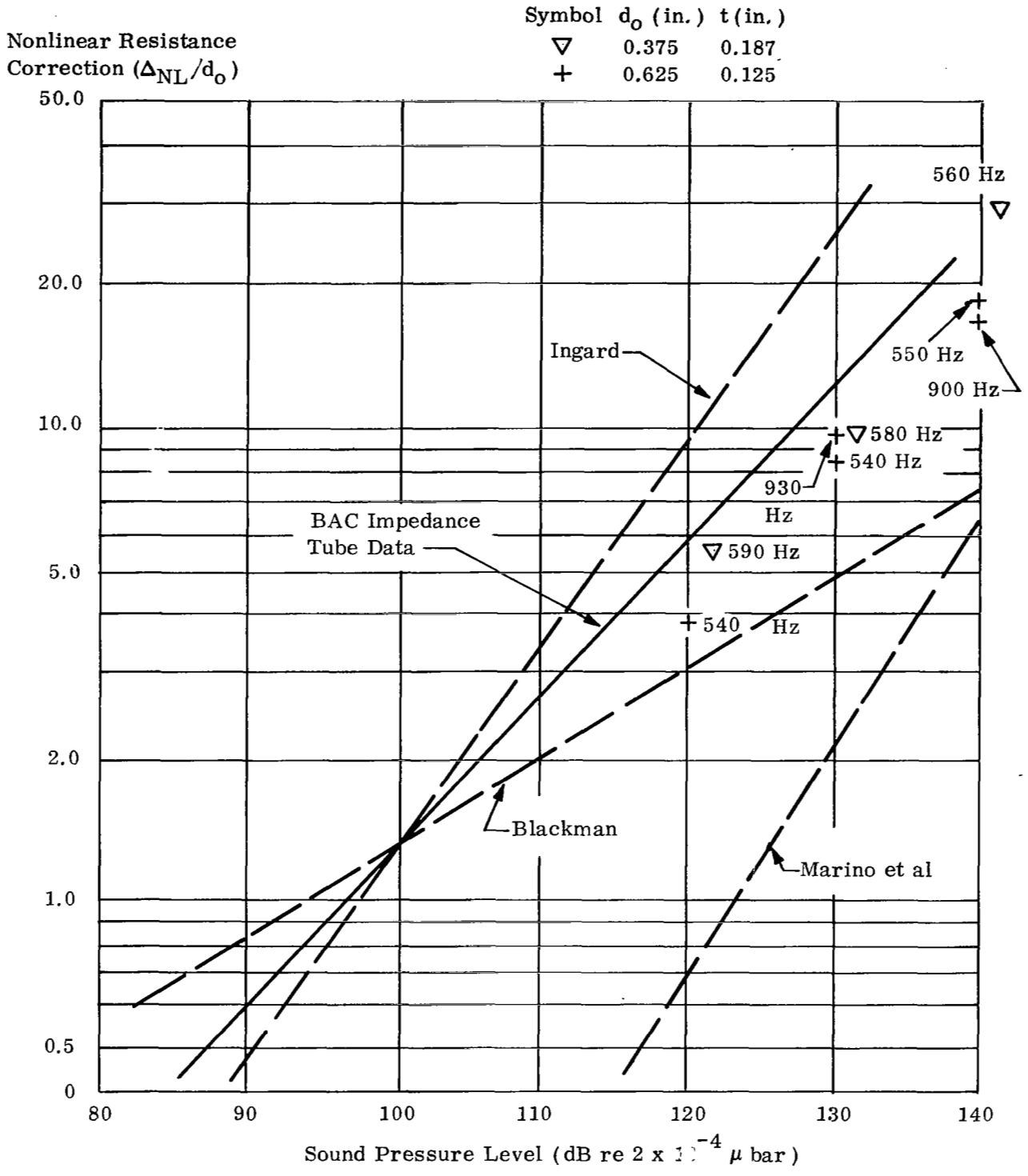

Figure 15. Comparison of Propeller Duct and Impedance Tube Resonator Data

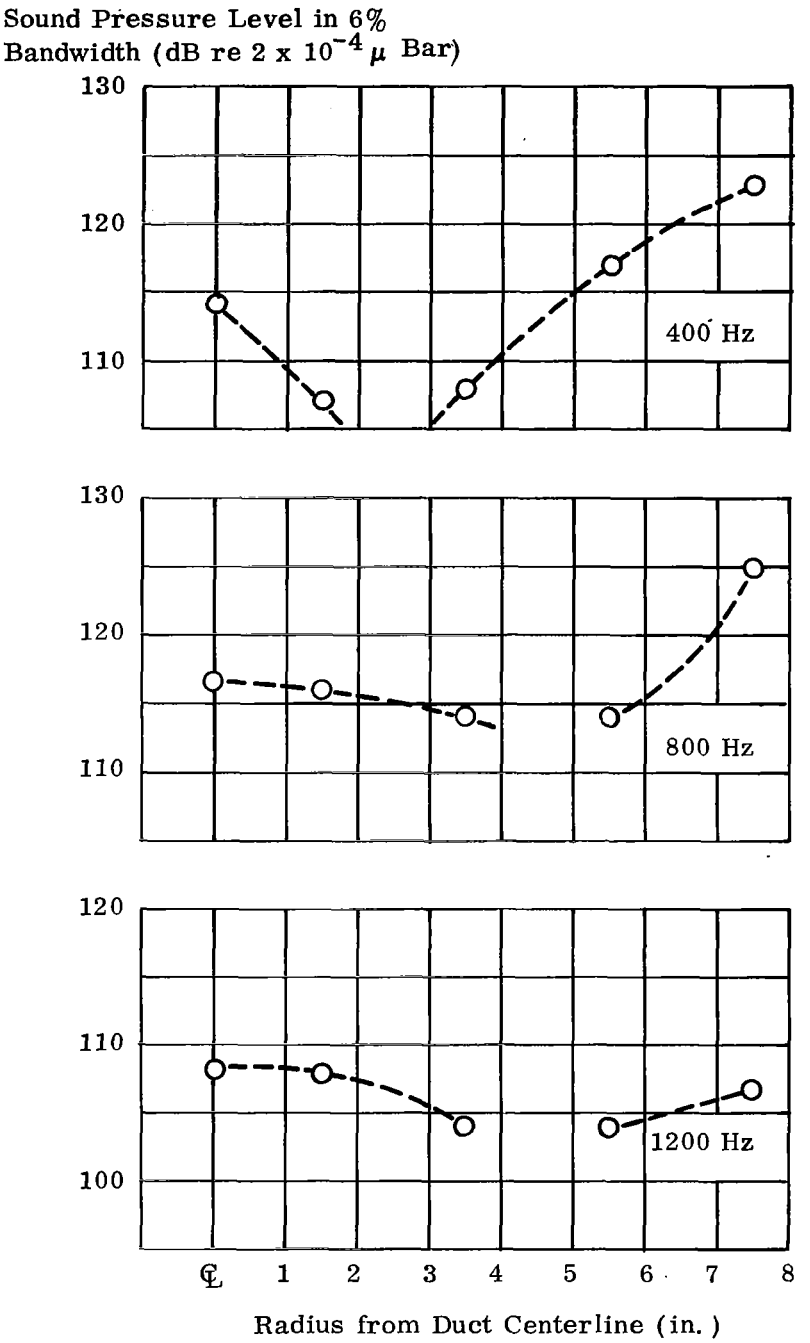

Figure 16. Radial Distribution of Sound Level in Duct No. 2 (Axial Location: 7.75 in.) Resonator Orifice Size: 0.625 in.diameter, 0.125 in. thick, f_{res} = 800 Hz

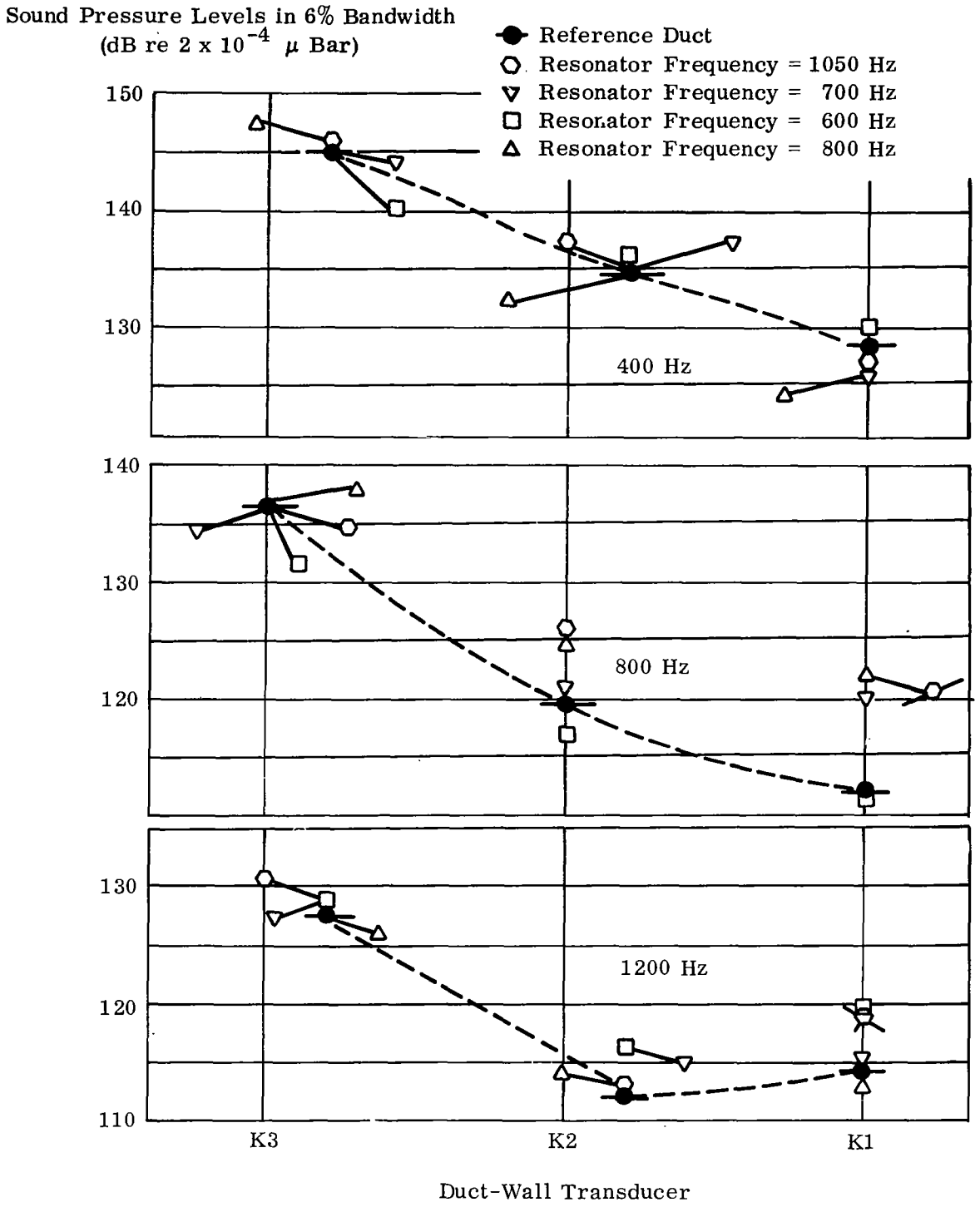

Figure 17. Duct-Wall Harmonic Levels With Resonators Tuned To Various Frequencies

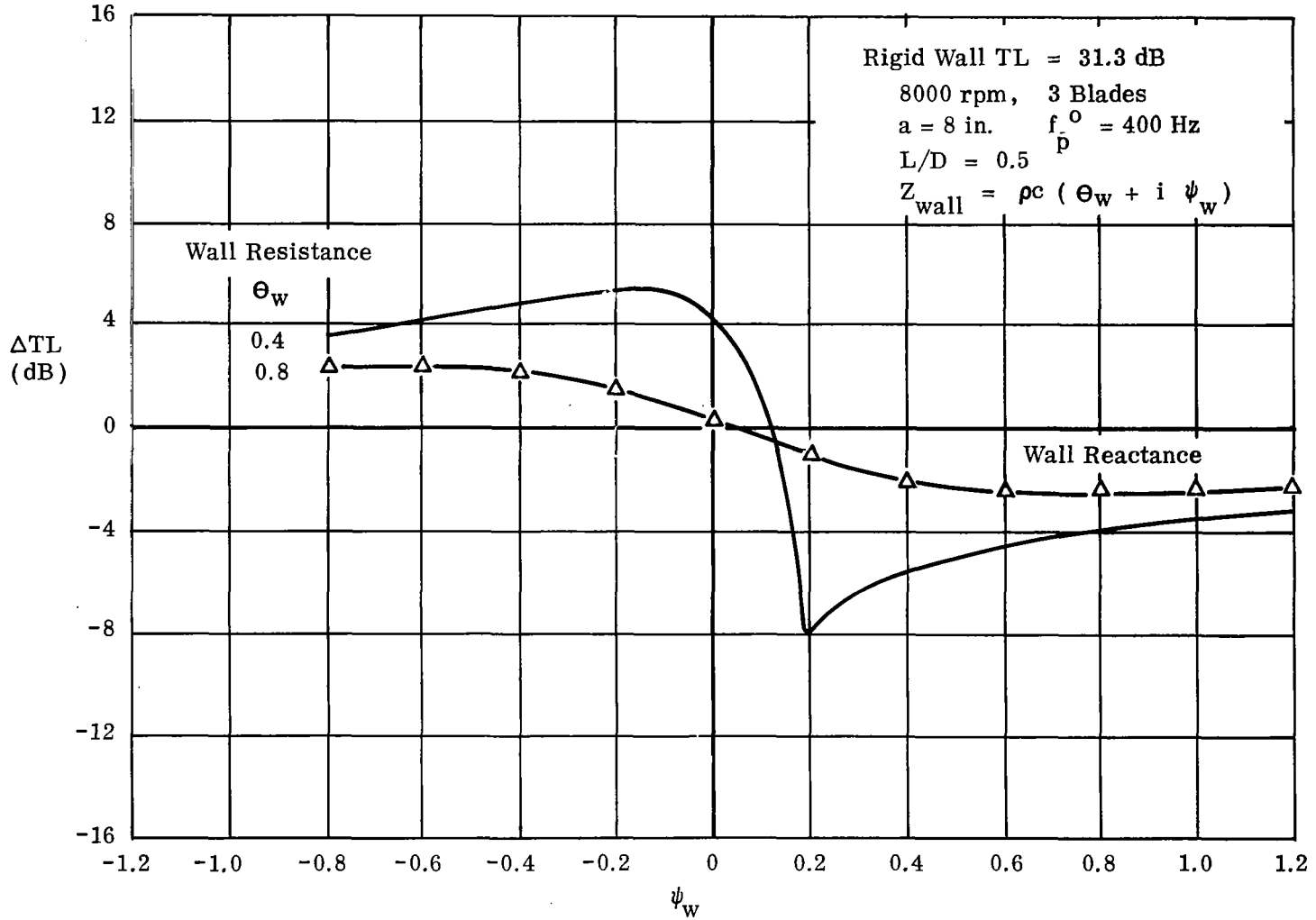

Figure 18. Theoretical Change in TL (dB) due to Finite Impedance for (0,1) Mode in Duct

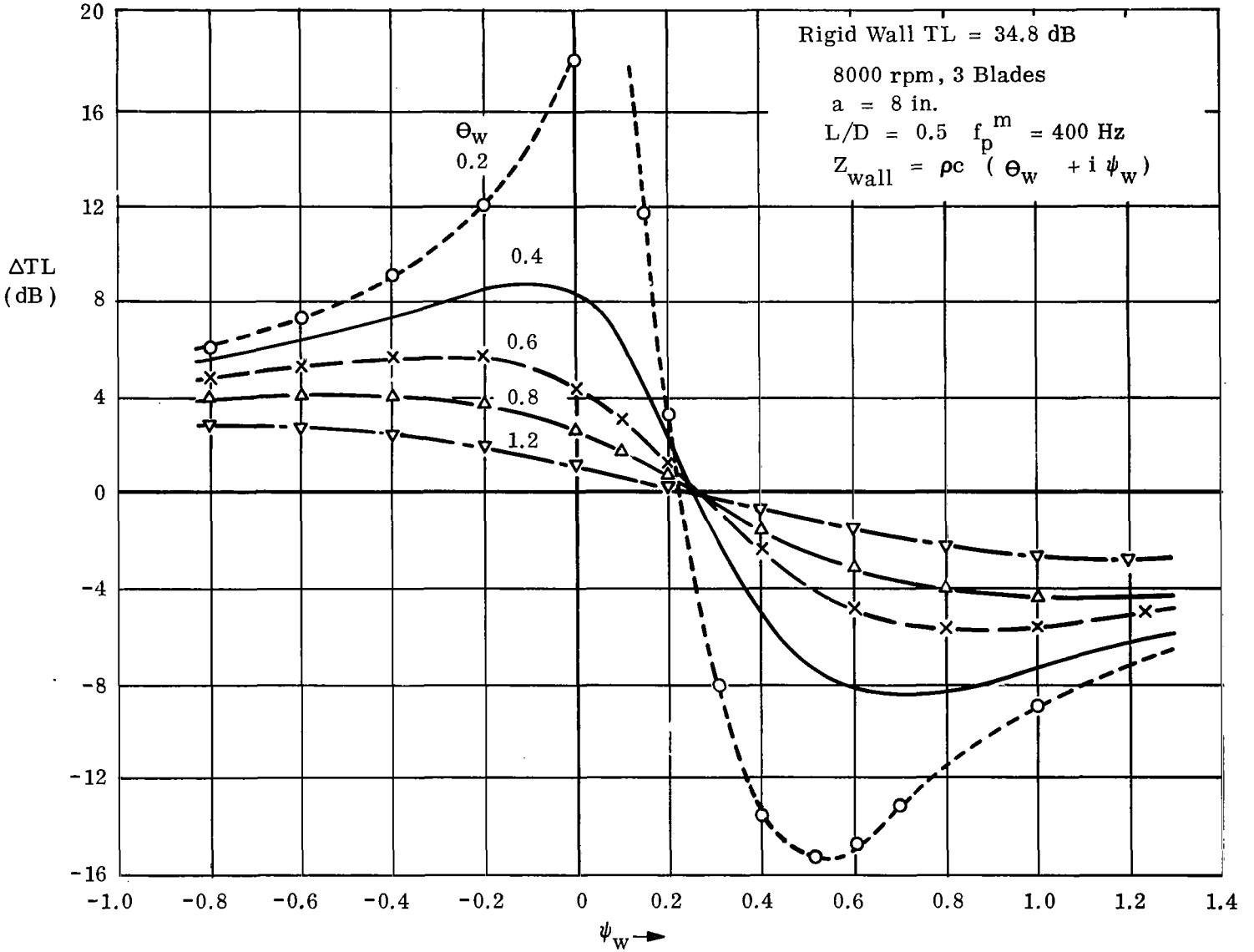

Figure 19. Theoretical Change in TL (dB) due to Finite Wall Impedance, for (3,0) Mode in Duct

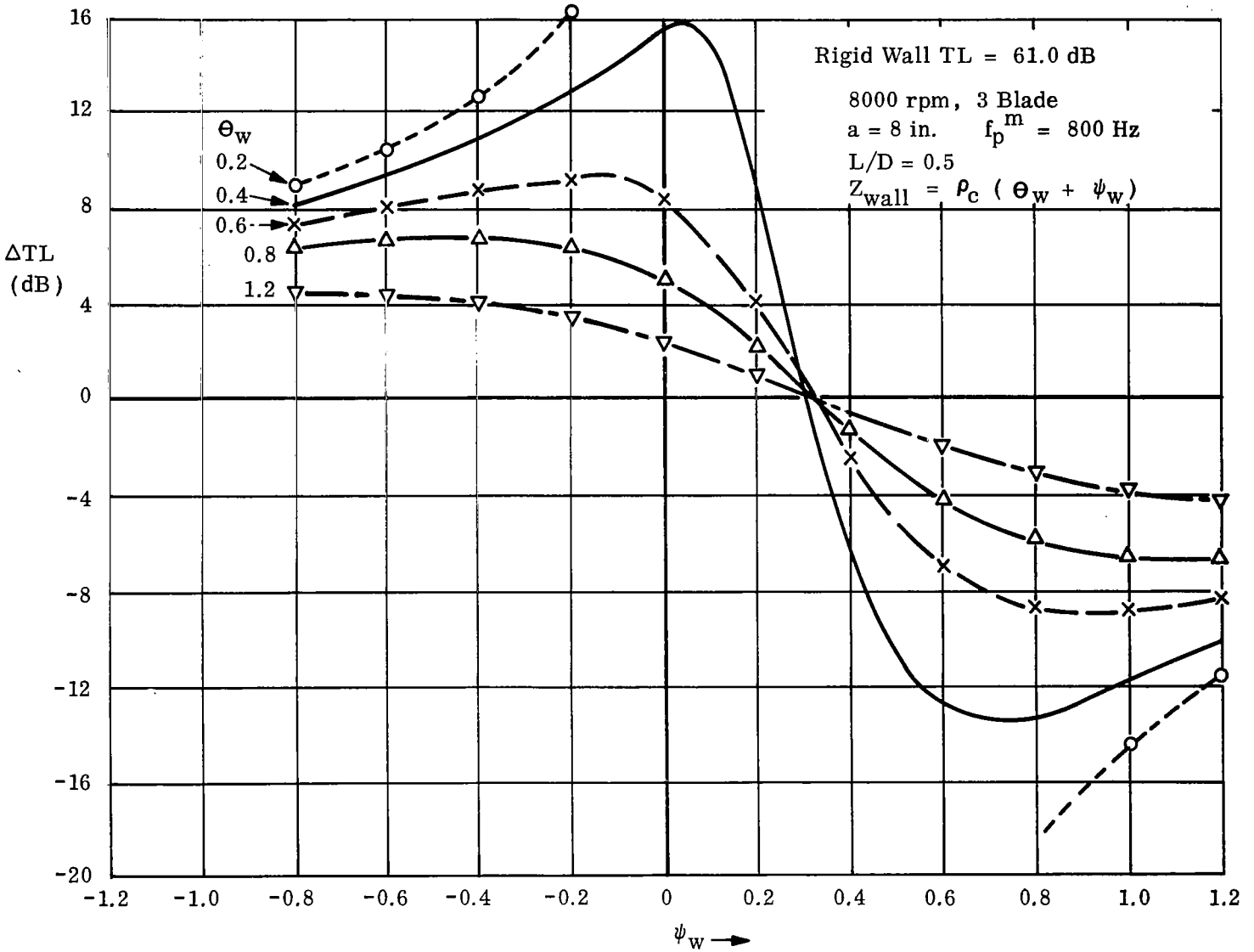

Figure 20. Theoretical Change in TL (dB) due to Finite Wall Impedance for (6.0) Mode in Duct